

1  
2  
3  
4  
5 **A silent disco: Persistent entrainment of low-frequency neural oscillations underlies**  
6 **beat-based, but not pattern-based temporal expectations**  
7

8 Short title: Persistent effects of beat- and pattern-based temporal expectations  
9

10 Fleur L. Bouwer<sup>1,2,3\*</sup>, Johannes J. Fahrenfort<sup>1,3</sup>, Samantha K. Millard<sup>3,4,5</sup>, Niels A.  
11 Kloosterman<sup>6,7</sup>, & Heleen A. Slagter<sup>1,3</sup>  
12  
13

14 <sup>1</sup> Department of Experimental and Applied Psychology, Institute Brain and Behavior  
15 Amsterdam (IBBA), Vrije Universiteit Amsterdam

16 <sup>2</sup> Institute for Logic, Language and Computation (ILLC), University of Amsterdam

17 <sup>3</sup> Department of Psychology, Amsterdam Brain and Cognition (ABC), University of  
18 Amsterdam

19 <sup>4</sup> Centre for Pain IMPACT, Neuroscience Research Australia (NeuRA), Sydney, New South  
20 Wales, Australia

21 <sup>5</sup> Faculty of Medicine, University of New South Wales (UNSW), Sydney, New South Wales,  
22 Australia

23 <sup>6</sup> Max Planck UCL Centre for Computational Psychiatry and Ageing Research, Berlin,  
24 Germany

25 <sup>7</sup> Center for Lifespan Psychology, Max Planck Institute for Human Development, Berlin,  
26 Germany

27  
28 \* Correspondence concerning this article should be addressed to Dr. Fleur Bouwer,  
29 Department of Psychology, University of Amsterdam (bouwer@uva.nl)

30  
31 FLB is supported by an ABC Talent Grant awarded by Amsterdam Brain and Cognition, a Veni  
32 grant awarded by the Dutch Research Council NWO (VI.Veni.201G.066), and the ERC starting  
33 grant awarded to HAS. HAS is supported by a European Research Council (ERC) starting grant  
34 (679399).  
35

36

## Highlights

37 - Temporal expectations can be based on both regular beats and predictable patterns

38 - Behavioral effects differentiate between beat-based and pattern-based expectations

39 - EEG power tracks the beat, but not the pattern, outlasting rhythmic stimuli

40 - Pattern-based and beat-based expectations differentially affect evoked potentials

41 - Decoding and entropy may index temporal expectations in a time-resolved way

42

43

## Abstract

44 The brain uses temporal structure in the environment, like rhythm in music and speech,  
45 to predict the timing of events, thereby optimizing their processing and perception. Temporal  
46 expectations can be grounded in different aspects of the input structure, such as a regular beat  
47 or a predictable pattern. One influential account posits that a generic mechanism underlies beat-  
48 based and pattern-based expectations, namely entrainment of low frequency neural oscillations  
49 to rhythmic input, while other accounts assume different underlying neural mechanisms. Here,  
50 we addressed this outstanding issue by examining EEG activity and behavioral responses  
51 during silent periods following rhythmic auditory sequences. We measured responses  
52 outlasting the rhythms both to avoid confounding the EEG analyses with evoked responses, and  
53 to directly test whether beat-based and pattern-based expectations persist beyond stimulation,  
54 as predicted by entrainment theories. To properly disentangle beat-based and pattern-based  
55 expectations, which often occur simultaneously, we used non-isochronous rhythms with a beat,  
56 a predictable pattern, or random timing. In Experiment 1 ( $N = 32$ ), beat-based expectations  
57 affected behavioral ratings of probe events for two beat-cycles after the end of the rhythm,  
58 while the effects of pattern-based expectations reflected one interval. In Experiment 2 ( $N = 27$ ),  
59 using EEG, we found enhanced spectral power at the beat frequency for beat-based sequences  
60 both during listening and the silence, but for pattern-based sequences, enhanced power at a  
61 pattern-specific frequency was only present during listening, not silence. Moreover, we found  
62 a difference in the evoked signal following pattern-based and beat-based sequences. Finally,  
63 we show how multivariate pattern decoding and multi scale entropy – measures sensitive to  
64 non-oscillatory components of the signal – can be used to probe temporal expectations.  
65 Together, our results suggest that different mechanisms implement temporal expectations,  
66 depending on the input structure. We suggest climbing activity may reflect pattern-based, and  
67 persistent low frequency oscillations beat-based expectations specifically.

68 *Keywords:* Temporal expectations, EEG, rhythm, entrainment, decoding, entropy

69

70

## Introduction

71 Predicting the timing of incoming events optimizes processing in our dynamic environment  
72 (Nobre & van Ede, 2018), as it allows the brain to increase sensitivity to events at predicted  
73 times (Auksztulewicz, Myers, Schnupp, & Nobre, 2019), without the need for constant  
74 vigilance (Breska & Deouell, 2017; Rimmele, Morillon, Poeppel, & Arnal, 2018; Schroeder &  
75 Lakatos, 2009b, 2009a). Entrainment models (Large & Jones, 1999) provide a mechanistic  
76 explanation for temporal expectations, by assuming that the phase and period of low-frequency  
77 neural oscillations synchronize to external rhythmic stimulation, causing optimal neural  
78 excitability at expected times (Haegens & Zion Golumbic, 2018; Henry & Herrmann, 2014;  
79 Schroeder & Lakatos, 2009a). In line with this, behavioral performance is improved for events  
80 in phase with an external rhythm (Bouwer & Honing, 2015; Herbst, Stefanics, & Obleser, 2022;  
81 Jones, Moynihan, MacKenzie, & Puente, 2002; Large & Jones, 1999), behavioral responses  
82 depend on the phase of delta oscillations (Arnal, Doelling, & Poeppel, 2014; Cravo, Rohenkohl,  
83 Wyart, & Nobre, 2013; Henry, Herrmann, & Obleser, 2014; Henry & Obleser, 2012), and low  
84 frequency oscillations phase lock to rhythmic input (Doelling, Assaneo, Bevilacqua, Pesaran,  
85 & Poeppel, 2019; Nozaradan, Peretz, Missal, & Mouraux, 2011; Stefanics et al., 2010).

86 Entrainment has mainly been studied in the context of periodic (“beat-based”) sensory  
87 input, but temporal expectations can also be based on memory for absolute intervals (Breska &  
88 Deouell, 2017; Breska & Ivry, 2016; Morillon, Schroeder, Wyart, & Arnal, 2016; Teki, Grube,  
89 Kumar, & Griffiths, 2011), either in isolation (“cue-based”), or as part of a predictable pattern  
90 of intervals (“pattern-based”, see (Nobre & van Ede, 2018)). Predictable temporal patterns may  
91 be especially important in speech and non-Western music, which is not necessarily periodic.  
92 Expectations based on predictable patterns in aperiodic sequences afford similar behavioral  
93 benefits as expectations based on a beat (Bouwer, Honing, & Slagter, 2020; Heideman, van  
94 Ede, & Nobre, 2018; O'Reilly, McCarthy, Capizzi, & Nobre, 2008), but pose a possible

95 challenge for entrainment models, which are arguably better suited to explain temporal  
96 expectations for periodic input (Breska & Deouell, 2017; Rimmele et al., 2018). Some have  
97 suggested that entrainment models can account for pattern-based expectations by assuming  
98 multiple coupled oscillators at different frequencies and with different phases (Tichko & Large,  
99 2019), or by assuming flexible top-down phase resets at expected moments, though this would  
100 entail some top-down mechanism, making observed entrainment the consequence, rather than  
101 the cause of expectations (Meyer, Sun, & Martin, 2019; Obleser & Kayser, 2019; Rimmele et  
102 al., 2018).

103 Alternatively, however, pattern-based and beat-based expectations could arise from  
104 dissociable neural mechanisms. For cue-based expectations, tentative evidence for a different  
105 underlying mechanism comes from a series of studies looking at the contingent negative  
106 variation (CNV), an event-related potential (ERP) component that peaks at expected moments  
107 (Praamstra, Kourtis, Kwok, & Oostenveld, 2006). The CNV resolved faster for beat-based than  
108 cue-based expectations (Breska & Deouell, 2017), and cerebellar patients showed selective  
109 impairments in forming cue-based, but not beat-based expectations (Breska & Ivry, 2018,  
110 2020). However, in these studies, the intended beat-based sequences were isochronous.  
111 Isochronous sequences can, in addition to a beat, elicit temporal expectations through learning  
112 the repeated, identical interval (Breska & Ivry, 2016; Keele, Nicoletti, Ivry, & Pokorny, 1989).  
113 Thus, the differences in responses may here be explained by more precise cue-based or pattern-  
114 based expectations in the isochronous, beat-based condition. Moreover, these studies tested  
115 temporal expectations based on the contingency between a cue and an interval (e.g., learning a  
116 single interval), and it is unclear whether temporal expectations based on patterns are based on  
117 the same mechanism (Nobre & van Ede, 2018). In our own recent work, we specifically  
118 compared beat-based and pattern-based expectations, and we found no difference in the effects  
119 of these expectations on early auditory ERP responses, suggestive of similar modulation of

120 sensory processing (Bouwer et al., 2020), but we observed suppression of sensory processing  
121 of unexpected events in beat-based rhythms, even when these events were fully predictable  
122 based on their pattern, suggesting different underlying mechanisms (Bouwer et al., 2020).  
123 However, in this study, we did not directly probe and contrasted the neural mechanisms  
124 underlying beat-based and pattern-based expectations, rendering it unclear whether they are  
125 subserved by shared or separate neural dynamics.

126 In the current study, we directly examined the role of entrainment in beat-based and  
127 pattern-based expectations, using non-isochronous rhythms designed to properly disentangle  
128 these two types of expectations. When studying entrainment, an important challenge has been  
129 to differentiate between real entrainment (“in the narrow sense”, see Obleser & Kayser, 2019)  
130 and regular evoked potentials, or similar phase locked responses that resemble entrainment with  
131 common analysis techniques (Zoefel, ten Oever, & Sack, 2018), and that may not differentiate  
132 between beat-based and memory-based expectations (Breska & Deouell, 2017). Crucially, to  
133 sidestep these issues, here we examined responses in a silent window after cessation of the  
134 rhythmic input, directly testing the prediction of entrainment models that entrainment should  
135 outlast sensory stimulation (Haegens & Zion Golumbic, 2018; Obleser & Kayser, 2019; Pesnot  
136 Lerousseau, Trébuchon, Morillon, & Schön, 2021; Zoefel et al., 2018).

137 Behaviorally, persistent entrainment has been shown for auditory rhythm (Hickok,  
138 Farahbod, & Saberi, 2015; Jones et al., 2002), though this effect is not always found (Bauer,  
139 Jaeger, Thorne, Bendixen, & Debener, 2015; Lin et al., 2021), possibly due to heterogeneity in  
140 the population and effects of musical training (Assaneo et al., 2019; Cameron & Grahn, 2014;  
141 Sun, Michalareas, & Poeppel, 2021). At a neural level, several studies reported persistent  
142 entrainment in the visual (de Graaf et al., 2013; Mathewson et al., 2012), and auditory (Kösem  
143 et al., 2018; Pesnot Lerousseau et al., 2021; van Bree, Sohoglu, Davis, & Zoefel, 2021; Wilsch,  
144 Mercier, Obleser, Schroeder, & Haegens, 2020) domain. However, in these studies,

145 isochronous stimuli were used, making it unclear whether the expectations probed were based  
146 on a beat, or were formed based on the single repeating interval (i.e., cue- or pattern-based).  
147 Moreover, persistent entrainment was not specific to the frequency of the input (Wilsch et al.,  
148 2020), or only occurred in the gamma (Pesnot Lerousseau et al., 2021), or alpha ranges (de  
149 Graaf et al., 2013; Mathewson et al., 2012), while humans have a preference for forming  
150 temporal expectations at slower rates (Ding et al., 2017; Merchant, Grahn, Trainor, Rohrmeier,  
151 & Fitch, 2015; Zalta, Petkoski, & Morillon, 2020), as naturally present in speech and music  
152 (i.e., the delta and theta range). Thus, not only is evidence for whether entrainment can account  
153 for pattern-based expectations lacking, evidence for persistent entrainment in response to beat-  
154 based rhythms remains elusive as well.

155 In the current study, participants listened to non-isochronous auditory sequences  
156 (similar to those used in Bouwer et al., 2020) with either a regular beat (eliciting beat-based  
157 expectations), a predictable pattern (eliciting pattern-based expectations), or random timing (no  
158 expectations). The non-isochronous beat-based sequences had a varying surface structure,  
159 similar to patterns used to probe beat-based processing in many neuroimaging (Grahn & Brett,  
160 2007; Grahn & Rowe, 2009; Leow & Grahn, 2014), behavioral (Bouwer et al., 2018, 2021;  
161 Cameron & Grahn, 2014; Povel & Essens, 1985), and electrophysiological studies (Lenc et al.,  
162 2021). While each beat was marked by a sound, between beats, sounds could occur at different  
163 times, or not at all. Therefore, the beat could not be extracted from the rhythmic signal by  
164 simply learning the transition of temporal intervals – as is possible in isochronous sequences.  
165 Moreover, in our previous study, using the same stimuli, we showed that the behavioral  
166 facilitation caused by introducing a regular beat was smaller than the facilitation caused by  
167 introducing a predictable pattern (Bouwer et al., 2020). Hence, the non-isochronous beat-based  
168 sequences used here did not allow for easy learning of the interval of the beat using a pattern-

169 based strategy, in contrast to the pattern-based sequences, in which the surface structure of the  
170 rhythm was fully predictable.

171 Each sequence was followed by a silent period. In Experiment 1, we asked participants  
172 to rate how well probe tones, presented at various time points during the silent period, fitted the  
173 preceding sequence. We expected the ratings to be affected by both the beat-based and pattern-  
174 based expectations elicited by the sequences. In Experiment 2, we recorded EEG activity both  
175 during presentation of the sequences and during the silence. If entrainment underlies temporal  
176 expectations, we should see persistent power at the frequency of the beat or pattern during the  
177 silence. Alternatively, if climbing activity in the form of a CNV underlies temporal  
178 expectations, we should see a CNV peaking at expected time points in the silence.

179 In addition to examining the spectral power at the frequencies of the beat and the pattern,  
180 and the evoked responses, we explored two new methods to index temporal expectations that  
181 do not rely on the EEG signal being a static oscillation. As recently argued, the oscillatory  
182 dynamics underlying such expectations may be subject to changes in power and frequency,  
183 depending on coupling between sound and brain, and on the properties of the neural dynamics  
184 themselves (e.g., to which extent the system shows damping of an oscillation without input, see  
185 Doelling & Assaneo, 2021). Once the rhythmic sensory input ceases, the oscillatory activity in  
186 the brain may quickly return to an intrinsic resonance frequency (Doelling & Assaneo, 2021).  
187 Also, the presence of non-sinusoidal recurring activity may not be captured by traditional  
188 analyses relying on Fourier transforms (Donoghue, Schawronkow, & Voytek, 2021), while it  
189 may be important for cognition (Waschke, Kloosterman, Obleser, & Garrett, 2021). Therefore,  
190 we here explore indexing temporal expectations in the silence using multi scale entropy (MSE)  
191 – a measure of signal irregularity (Kosciessa, Kloosterman, & Garrett, 2020) – and multivariate  
192 pattern decoding. These methods may provide useful tools to study the neural dynamics  
193 underlying rhythm processing and temporal expectations, which are often hard to study due to

194 methodological issues with analyzing the EEG signal (Zoefel et al., 2018). While MSE provides  
195 us with a method to look at possible non-sinusoidal contributions to the EEG signal related to  
196 temporal expectations, decoding allows us to look at how entrainment evolves over time. Note  
197 that we consider these analyses exploratory in nature, and results should be interpreted as such.

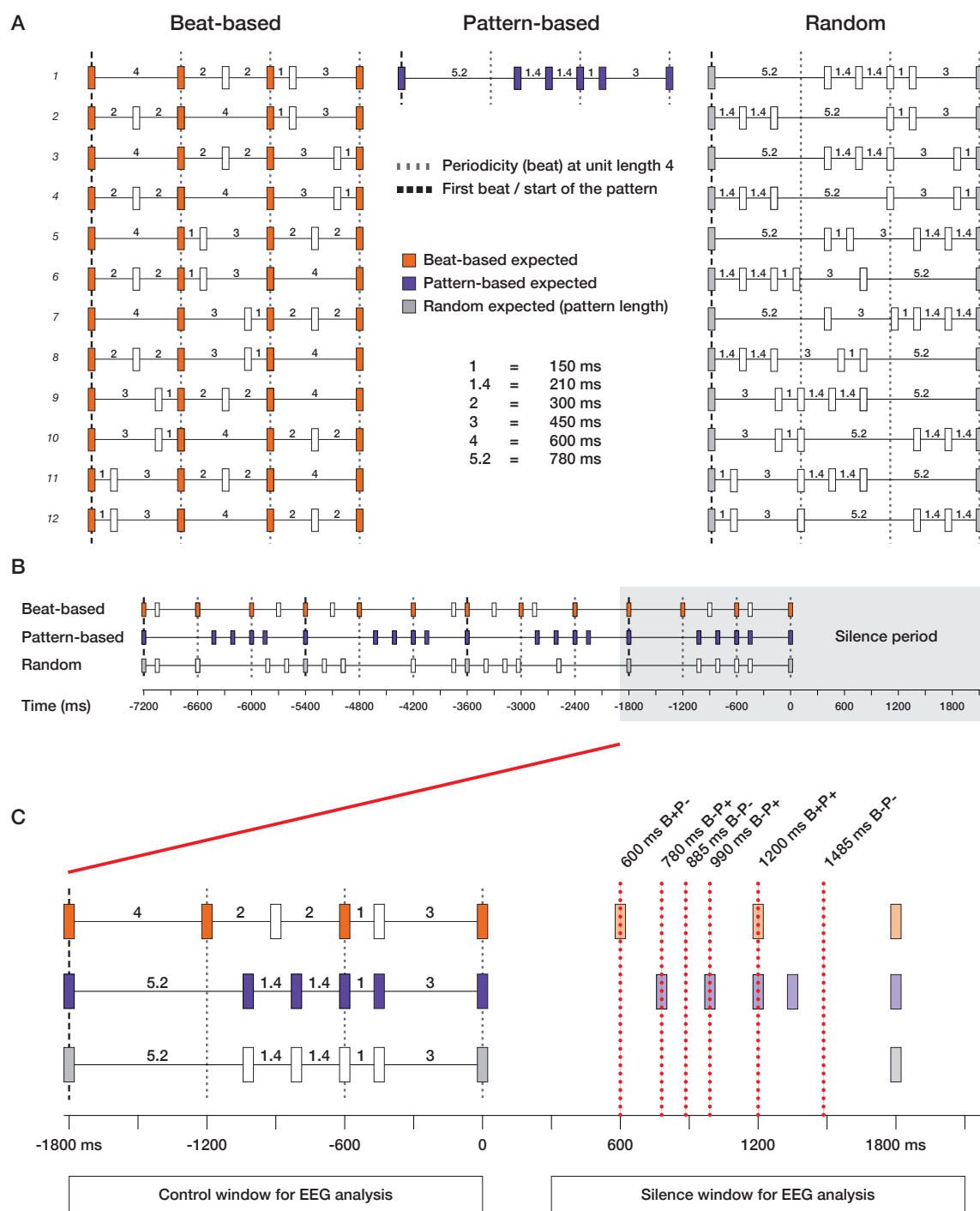
198

199

## Materials and methods

200 **Participants**

201 Thirty-two participants (18 women), aged between 18 and 44 years old ( $M = 24$ ,  $SD = 5.6$ ) took part in the behavioral Experiment 1, and 32 participants (26 women), aged between 202 19 and 28 years old ( $M = 23$ ,  $SD = 2.5$ ) took part in the EEG experiment (Experiment 2), in 203 exchange for course credit or monetary compensation. Due to technical problems, the EEG data 204 from five participants was not recorded correctly, hence we report the results for 27 participants 205 (21 women, between 19 and 28 years old,  $M = 23$ ,  $SD = 2.4$ ). For the behavioral experiments, 206 we used mixed-effects models, which need both the number of participants and the number of 207 items to be taken into account to assess power (Brysbaert & Stevens, 2018). In two similar 208 experiments in which ratings in response to rhythms of varying complexity were analyzed, 209 small-sized effects were replicated with a total number of around 275 responses per condition 210 (Bouwer, Burgoyne, Odijk, Honing, & Grahn, 2018). For our new experimental paradigm, we 211 here included a multiple of this amount of trials (960 responses per condition and probe position 212 in Experiment 1 – 32 participants with 30 responses each in each cell – and, after loss of data 213 was accounted for, 486 responses per condition and probe position in Experiment 2 – 27 214 participants and 18 responses per cell). Previous EEG experiments examining persistent 215 entrainment in the auditory domain used sample sizes ranging from fifteen (Pesnot Lerousseau 216 et al., 2021) to twenty-one (van Bree et al., 2021), similar to the sample size used in a study 217 looking at different types of temporal expectations (twenty-one, Breska & Deouell, 2017). To 218 obtain robust power, we here tested thirty-two participants, which, even when loss of data is 219 accounted for, thus exceeded typical sample sizes as used previously. None of the participants 220 reported a history of hearing or neurological problems, and all provided written informed 221 consent prior to the onset of the study. The experiment was approved by the Ethics Review 222 Board of the Faculty of Social and Behavioral Sciences of the University of Amsterdam.



224

225 **Figure 1. Schematic overview of the rhythmic stimuli used and the task.** A) Twelve patterns of five  
 226 temporal intervals with integer ratio durations and an event at each 600 ms period were created to form beat-  
 227 based sequences. Equivalent patterns without a regular beat every 600 ms were created by using non-integer  
 228 ratio durations, while keeping the number of intervals and grouping structure the same (random condition).  
 229 For the pattern-based sequences, only pattern 1 was used, to allow for learning of the intervals. B) Four semi-  
 230 randomly chosen patterns were concatenated to form rhythmic sequences. In both the beat-based and random  
 231 sequences, the last pattern was always pattern 1 or 2, to equate the acoustic context preceding the silent  
 232 period. C) To measure behavioral effects of expectations, a probe tone could appear at various temporal  
 233 positions in the silent period (indicated by the dashed red lines), predictable based on a beat (B+, light  
 234 orange), predictable based on the pattern (P+, light purple), or unpredictable based on the beat (B-) or pattern  
 235 (P-). Subjects had to indicate how well the probe tone fitted the preceding rhythm. In Experiment 1, all 6  
 236 probe tone positions were used. In Experiment 2, only the last 3 probe positions were used.

237 ***Stimuli***

238 We used patterns marked by woodblock sounds of 60 ms length, generated in  
239 GarageBand (Apple Inc.), as previously used in (Bouwer et al., 2020) to elicit beat-based and  
240 pattern-based expectations (Figure 1). Each pattern was 1800 ms long and consisted of five  
241 temporal intervals. The number of tones was chosen to be within the range that was previously  
242 shown to allow for learning of a predictable pattern (Schultz, Stevens, Keller, & Tillmann,  
243 2013), while the length of the pattern was such that the formation of beat-based expectations  
244 with a period of the entire pattern would be unlikely in the pattern-based sequences, given that  
245 this would require hearing a beat at 0.55 Hz, which is very far from the range at which humans  
246 can typically perceive a beat (Honing & Bouwer, 2019; London, 2012). Sequences (beat-based,  
247 pattern-based, or with random timing) were constructed by concatenating four patterns and a  
248 final tone, for a total sequence length of 7260 ms (four patterns of 1800 ms, plus 60 ms for the  
249 final tone).

250 In the twelve patterns used to create beat-based sequences (Figure 1), temporal intervals  
251 were related to each other with integer-ratio durations. The shortest interval had a length of 150  
252 ms, with the relation between the five intervals used of 1:2:2:3:4 (i.e., 150, 300, 300, 450, and  
253 600 ms). The sounds were grouped such that a perceptually accented sound (Povel &  
254 Okkerman, 1981) occurred every 600 ms (every unit length 4), giving rise to a beat at 100 beats  
255 per minute, or 1.67 Hz, within the range of preferred tempo for humans (London, 2012). All  
256 beat-based patterns were strictly metric, with the beat always marked by a sound (Grahn &  
257 Brett, 2007). Sequences of beat-based patterns were constructed from four semi-randomly  
258 chosen patterns, with the restriction that the last pattern of the sequences was always pattern 1  
259 or 2 (see Figure 1). This way, the final 600 ms preceding the silence epoch was equated in terms  
260 of the acoustic context, to make the bleed of auditory ERPs into the silence as similar between  
261 conditions as possible. Note that in beat-based sequences, a sound could be expected every 600

262 ms based on the beat, but the surface structure of the pattern was unpredictable, due to the  
263 random concatenation of patterns.

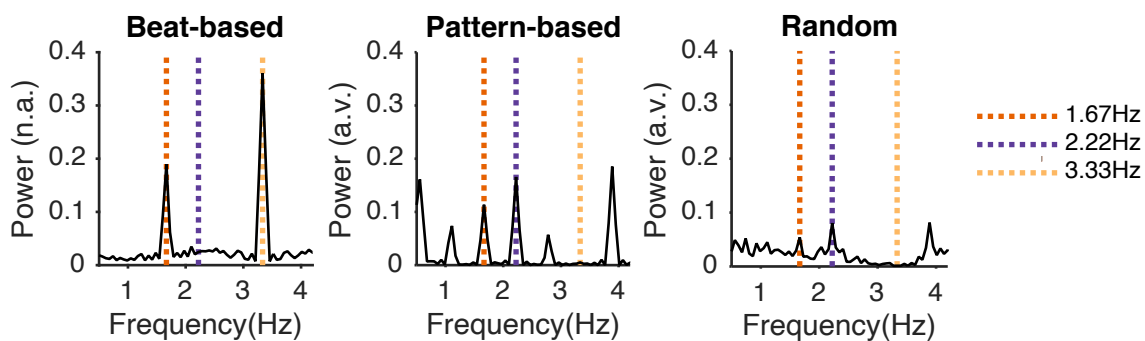
264 To create patterns that did not allow for beat-based expectations (“aperiodic” patterns,  
265 see Figure 1), the ratios by which the temporal intervals were related were changed to be non-  
266 integer (1:1.4:1.4:3:5.2, or 150, 210, 450, and 780 ms respectively). In these patterns, no marked  
267 beat was present at unit length four, nor at any other subdivision of the 1800 ms pattern (Bouwer  
268 et al., 2020), while the patterns were matched to their periodic counterparts in terms of overall  
269 length, event density, number of sounds, and grouping structure.

270 From the aperiodic patterns, two types of sequences were created: pattern-based and  
271 random sequences. To create sequences allowing for pattern-based expectations, we  
272 concatenated four identical patterns. To be able to use the data with an EEG-based decoding  
273 analysis (Experiment 2), we needed the timing of expectations in the silence to be identical for  
274 each sequence, hence we restricted the pattern-based sequences to only pattern 1. The use of a  
275 single pattern was not only necessary for decoding, but also optimized the experiment for  
276 pattern-based expectations, since participants only had to memorize one pattern, allowing them  
277 to easily form expectations, even if the single sequences were only four patterns long.

278 For the random sequences, four semi-randomly chosen aperiodic patterns were  
279 concatenated. Like for the beat-based sequences, the final pattern was always pattern 1 or 2,  
280 equating the final 600 ms of the sequences in terms of acoustics. In the random sequences, the  
281 timing of sounds could not be predicted based on the surface structure of the pattern, nor on the  
282 basis of an underlying beat.

283 A spectral analysis of the stimuli in the range in which a beat can normally be perceived  
284 (the delta-range, 0.5-4 Hz) confirmed that in the beat-based sequences, a peak was present at  
285 the beat frequency of 1.67 Hz as well as at 3.33 Hz (see Figure 2). The 3.33 Hz peak is a  
286 harmonic of the beat frequency, but also the frequency at which participants may perceive

287 subdivisions of the beat (e.g., an extra layer of perceived metrical regularity with a period of  
288 300 ms). In the pattern-based and random sequences, peaks were more distributed, in line with  
289 the more irregular nature of these rhythms, and the highest peaks in the delta range were at 2.22  
290 and 3.89 Hz.



292 **Figure 2. Spectral analysis of the sound signal of the different rhythmic sequences.** Ten sequences per  
293 condition were generated to base the spectral analysis on. Note that these sequences were identical for the  
294 pattern-based condition, but semi-random for the beat-based and random conditions. The envelope of each  
295 sequence was obtained by performing a Hilbert transform, and subsequently, a fast fourier transform (fft)  
296 was used to obtain the spectral decomposition and power values were averaged over ten sequences. n.a.=  
297 normalized amplitude.

298

299 In Experiment 1, to assess the persistence of temporal expectations behaviorally, on  
300 each trial, a probe tone was presented at 600, 780, 885, 990, 1200, or 1485 ms after the onset  
301 of the last tone of the sequence (see Figure 1C), and participants provided ratings for how well  
302 probe tones fitted the preceding rhythm. These positions were carefully chosen to represent  
303 times at which a tone could be expected based on the beat (600, 1200 ms), based on memory  
304 for the pattern (780, 990, 1200 ms), or neither (885, 1485 ms). Note that the latter two probe  
305 tones that were unexpected based on the beat (780, 885, 990, and 1485 ms) did not fall on  
306 subdivisions of the beat.

307 Experiment 2 contained both trials in which a probe tone was presented (25% of the  
308 trials, using only the last three probe positions), and trials in which a 7260 ms sequence was  
309 followed by a silence period without a probe tone (75% of the trials). The latter were used for  
310 EEG analyses, uncontaminated by a probe presentation. The silent period lasted for 2100 ms

311 after the onset of the last sound, providing 300 ms immediately following the final sound to  
312 allow for ERPs to mostly return to baseline, and 1800 ms (three full beat cycles, or a full cycle  
313 of the repeating pattern) of silence for the analysis. After the silence, the onset of the next  
314 sequence was jittered between 25 and 75 ms to prevent carryover of the beat from previous  
315 sequences (e.g., the next trial started between 325 and 375 ms after the last beat in the silence,  
316 which is not on the beat, nor at a subdivision of the beat). On trials that contained a probe tone,  
317 we chose to only use the last three probe positions, to 1) limit the time for the EEG experiment  
318 to prevent fatigue, 2) still provide participants with the incentive to form expectations well into  
319 the silence period, as a probe tone could appear as late as 1485 ms into the trial, and 3) obtain  
320 some measure of whether participants formed expectations, by including positions that were  
321 expected based on the beat and the pattern (1200 ms), based on the pattern only (990 ms) or  
322 neither (1485 ms).

### 323 ***Procedure***

324 Participants were tested individually in a dedicated lab at the University of Amsterdam.  
325 Upon arrival, participants were provided with information about the experiment, provided  
326 written informed consent, and were allowed to practice the task. On probe tone trials (all trials  
327 in Experiment 1, 25% of the trials in Experiment 2), participants were asked to judge on a four-  
328 point scale (“very poorly”, “poorly”, “well”, “very well”) how well the probe tone fitted the  
329 preceding sequence, similar to previous studies investigating the perception of musical meter  
330 (Manning, Harris, & Schutz, 2017; Manning & Schutz, 2013; Palmer & Krumhansl, 1990).  
331 Participants could respond with four buttons on the armrest of their chair, two on each side. The  
332 order of the answer options on the screen in front of the participants was randomized on each  
333 trial, to avoid any artefacts of motor preparation in participants that anticipated which answer  
334 they would provide. There was no time limit for responses and the next trial started after a  
335 response was made.

336            In Experiment 1, each participant was presented with 18 blocks of 30 trials, amounting  
337            to 540 trials in total (30 trials per probe position for each condition). In Experiment 2,  
338            participants were presented with 18 blocks of 36 trials, for a total of 648 trials (18 per condition  
339            and position). In Experiment 2, for each condition, 162 trials were silence trials, and did not  
340            contain a probe tone. Fifty-four trials for each condition contained a probe tone. In both  
341            experiments, in each block, only one type of sequence (beat-based, pattern-based, or random)  
342            could appear to optimize for the formation of expectations. Blocks were semi-randomized, with  
343            each type appearing once in a set of three blocks. In each block of Experiment 2, the number  
344            of probe trials was varied between 3 and 11, for an average of 25% probe trials, and 75% silent  
345            trials.

346            Sounds were presented through a single speaker positioned in front of the participant  
347            using Presentation® software (version 14.9, [www.neurobs.com](http://www.neurobs.com)). After completion of the  
348            experiment, participants performed the Beat Alignment Task (Iversen & Patel, 2008;  
349            Müllensiefen, Gingras, Musil, & Stewart, 2014) to assess their beat perception abilities, and  
350            completed the musical training subscale from the Goldsmith Musical Sophistication Index  
351            (GMSI) questionnaire to assess their musical training (Müllensiefen et al., 2014). In total, a  
352            behavioral session lasted two hours, and the EEG session lasted between 3.5 and 4 hours.

353            ***Behavioral analysis***

354            A total of 17280 responses was included in the analysis of Experiment 1 (32 participants,  
355            3 conditions, 6 probe positions, 30 responses each), and 4374 in the analysis of Experiment 2  
356            (27 participants, 3 conditions, 3 probe positions, 18 responses each). To account for the ordinal  
357            nature of the Likert-scale responses (Bouwer et al., 2018; Carifio & Perla, 2008; Jamieson,  
358            2004), we used a mixed ordinal regression model. With this model, the ordinal responses are  
359            normalized, to correct for potential unequal distances between rating points. The results can  
360            subsequently be interpreted similar to the results from a normal mixed model regression. Two

361 independent variables and their interaction were included in the model as fixed factors:  
362 Condition (beat-based, pattern-based, or random), and Probe Position (600, 780, 885, 990,  
363 1200, or 1485 ms; only the latter three in Experiment 2). Additionally, the score on the GMSI  
364 musical training questionnaire was included as a continuous variable (Musical Training), as  
365 well as its interactions with the two fixed factors. We used a random intercept for each subject  
366 to account for between-subject variation.

367 The initial model showed a significant effect of Probe Position in the random condition,  
368 most likely due to recency effects. To assess the effect of Probe Position in the beat-based and  
369 pattern-based conditions while accounting for recency effects, for each participant we  
370 subtracted the mean response in the random condition at each position from the responses in  
371 the beat-based and pattern-based condition. Subsequently, we submitted the random-baseline-  
372 corrected ratings to a second ordinal regression model, with only two levels for the factor  
373 Condition (beat-based and pattern-based) and without the random intercept for each participant  
374 (as the baseline correction already corrected for between-subject variability). For both the  
375 original model, and the baseline corrected model, significant interactions were followed up by  
376 tests of simple effects, corrected for multiple comparisons using a Bonferroni correction.

377 The statistical analysis was conducted in R (R Development Core Team, 2008). The  
378 ordinal mixed model was implemented using the clmm() function from the ordinal package  
379 (Christensen, 2019). Subsequently, we used the Anova() function from the car package (Fox &  
380 Weisberg, 2019) to look at omnibus effects for the main factors of interest, and the emmeans  
381 package (Lenth, 2019) to assess simple effects and compare slopes between conditions.

382 ***EEG recording***

383 EEG was recorded at 1024 Hz using a 64-channel Biosemi Active-Two acquisition  
384 system (Biosemi, Amsterdam, The Netherlands), with a standard 10/20 configuration and

385 additional electrodes for EOG channels (located under and on the left and right sides of the  
386 eye), on the nose, on both mastoids, and on both earlobes.

387 ***EEG analysis***

388 Preprocessing was performed in MATLAB, version 2015a (Mathworks) and EEGLAB,  
389 version 14.1.1 (Delorme & Makeig, 2004). Data were offline down-sampled to 256 Hz, re-  
390 referenced to averaged mastoids, bad channels were manually removed, and eye-blanks were  
391 removed using independent component analysis. Subsequently, bad channels were replaced by  
392 values interpolated from the surrounding channels.

393 **ERPs.** For the ERP analysis, the continuous data were filtered using 0.1 Hz high-pass  
394 and 40 Hz low-pass finite impulse response filters (as implemented in the standard EEGLAB  
395 filter function `pop_eegfiltnew`). Epochs were extracted from the data from -1800 till 2100 ms  
396 relative to the onset of the last sound. Epochs with a voltage change of more than 150 microvolts  
397 in a 200 ms sliding window were rejected from further analysis. For each participant and  
398 condition, epochs were averaged to obtain the ERPs, and ERPs were averaged over participants  
399 to obtain grand average waveforms for plotting. All waveforms were initially baseline corrected  
400 using the average voltage of a 50 ms window preceding the onset of the last sound of the  
401 sequence. This baseline can be regarded as preceding the “cue” (the last event before the onset  
402 of the expectation). Such a baseline is customary in CNV analyses. However, visual inspection  
403 suggested that this baseline was biased, as baseline correction resulted in an overall shift of the  
404 waveform amplitude relative to each other, as also reflected in a significant cluster when  
405 comparing beat-based and pattern-based conditions that spanned the entire analysis epoch (see  
406 Supplementary Figure 1). This was likely caused by the rapid succession of sounds preceding  
407 the onset of the silence, which made it impossible to find a clean, unbiased baseline. Therefore,  
408 we repeated the analysis without baseline correction, to confirm that the results were not caused  
409 by a noisy baseline.

410 As a control analysis, we repeated the above analysis for the longest intervals during the  
411 presentation of the rhythmic streams, to assess whether in those longer intervals, we could  
412 observe similar deflections in the evoked potentials as observed in the silence. For this analysis,  
413 epochs were extracted from -200 till 880 ms around the onset of the sound preceding the long  
414 interval (600 ms in the beat-based condition, and 780 ms in the other conditions, see Figure 1).  
415 All preprocessing steps were identical to the analysis of the ERPs in the silence. The control  
416 analysis is reported in the Supplementary Materials (Supplementary Figure 1).

417 Three cluster-based permutation tests (Oostenveld, Fries, Maris, & Schoffelen, 2011)  
418 were used to compare all three conditions against each other (i.e., beat-based vs. random;  
419 pattern-based vs. random; beat-based vs. pattern-based), comparing all timepoints from 300 till  
420 1200 ms after the onset of the final sound for the silence (see Figure 1), and all timepoints from  
421 300 till 600 ms after the onset of the preceding sound for the long intervals during the sequences  
422 (as the next sound came in at 600 ms for the beat-based condition, we could not compare the  
423 conditions beyond this timepoint). This window excluded a large portion of the ERP response  
424 to the previous sound, and included both the first expected moments for beat-based (600 ms)  
425 and pattern-based (780 ms) expectations in the silence window, and additional time to allow  
426 for an evaluation of possible return to baseline of the CNV (Breska & Deouell, 2017). For the  
427 ERP analysis, clusters were formed based on adjacent time-electrode samples.

428 For all EEG analyses, cluster-based tests were evaluated statistically by forming clusters  
429 of samples based on dependent samples t-tests and a threshold of  $p < 0.05$ , and using  
430 permutation tests with 2000 permutations of the data. We report corrected  $p$ -values to account  
431 for two-sided testing (multiplied by a factor of two).

432 **Frequency-domain analysis.** To obtain the spectrum of the EEG signal in the silence,  
433 we used the raw, unfiltered data. Epochs were extracted from the continuous data both from -  
434 1800 till 0 ms relative to the onset of the last sound (control window, see Figure 1), and from

435 300 till 2100 ms relative to the onset of the last sound (silence window, see Figure 1), the latter  
436 starting at 300 ms to avoid contamination from the final ERPs. Both windows thus had equal  
437 length, both spanning three full cycles of the beat. Epochs with an amplitude change of 250  
438 microvolts or more in a sliding 200 ms window were rejected from further analysis. The more  
439 lenient rejection criterium compared to the ERP analysis was used to account for the fact that  
440 these data were unfiltered, and to avoid rejection of too many trials that showed some slow  
441 drift. All epochs were baseline corrected using the mean of the entire epoch. Subsequently,  
442 epochs were averaged for each condition separately to obtain the evoked signal, phase locked  
443 to the onset of the final sound, and similar to previous studies using frequency tagging to look  
444 at beat-based perception (Lenc et al., 2021; Nozaradan et al., 2011; Nozaradan, Peretz, &  
445 Mouraux, 2012).

446 For each participant and condition separately, the average waveforms were transformed  
447 into the frequency domain using an FFT, with the data zero-padded to 4608 samples (NFFT) to  
448 obtain a better frequency resolution (0.056 Hz), and importantly, be able to extract data at  
449 exactly the frequencies of interest. Note that the zero-padding can only improve the frequency  
450 resolution, but not the frequency precision, which by definition with the 1800 ms epochs is  
451 limited to 0.56 Hz. While the design of the experiment simply does not allow for a better  
452 resolution, the 0.56 Hz does allow us to differentiate between the frequencies of interest, which  
453 are 0.56 Hz or more apart. The obtained power values at each frequency were normalized to  
454 account for the 1/f distribution of noise (Nozaradan et al., 2011, 2012), by subtracting the  
455 average of neighboring bins four to six on either side for all frequencies (e.g., 1.33 – 1.44 Hz  
456 and 1.89 – 2.00 Hz for the beat frequency, 1.89 – 2.00 Hz and 2.44 – 2.56 Hz for the pattern-  
457 based frequency, and 3.00 – 3.11 Hz and 3.56 – 3.67 Hz for the beat subdivisions). To account  
458 for bleeding into neighboring frequency bins (Nozaradan et al., 2011, 2012), for each  
459 frequency, we averaged over 5 bins centered on that frequency (e.g., for the frequencies of

460 interest, this was 1.56 – 1.78 Hz for the beat frequency, 2.11 – 2.33 Hz for the pattern-based  
461 frequency, and 3.22 – 3.44 Hz for the beat subdivisions).

462 To statistically test differences between conditions in the evoked power at the  
463 frequencies of interest, we used cluster-based permutation tests. First, this avoided bias by  
464 selecting only a subset of electrodes, as we used all scalp electrodes, as was done in previous  
465 research (Lenc, Keller, Varlet, & Nozaradan, 2018; Nozaradan et al., 2011; Tal et al., 2017).  
466 Second, the permutation tests accounted for the non-normal distribution of the data. Like for  
467 the ERPs, we ran t-tests comparing the normalized data for all conditions and for each frequency  
468 of interest (e.g., those most prominent in the sound signal). We included the frequencies that  
469 showed the highest peaks in the spectral analysis of the sound (i.e. 1.67 Hz, 2.22 Hz, and 3.33  
470 Hz), except for 3.89 Hz, since a peak at this frequency was absent on visual inspection in the  
471 spectral decomposition of the EEG data. For the frequency-domain analysis, clusters were  
472 formed based on adjacent electrodes.

473 The cluster-based tests yielded null results for the pattern-based condition in the silence  
474 (e.g., there was no larger power at 2.22 Hz in the pattern-based than in the random condition,  
475 see Results). To quantify the possible absence of persistent entrainment for the pattern-based  
476 condition, we performed a Bayesian t test using JASP (JASP, 2019; Wagenmakers et al., 2018).  
477 We compared the power in the pattern-based and random conditions at 2.22 Hz in the silence,  
478 averaged over electrodes contributing to the significant cluster in the silence for the beat-based  
479 condition at 1.67 Hz, to optimize for finding entrainment effects. We estimated Bayes factors  
480 using a Cauchy prior distribution ( $r = .71$ ) and performed a robustness check to assess the effect  
481 of a different prior ( $r = 1$ ; see (Jeffreys, 1961; Wagenmakers et al., 2018)).

482 We performed an additional exploratory analysis to assess phase alignment directly.  
483 First, we computed inter-trial phase consistency for each participant, condition, and frequency  
484 of interest separately, by transforming single epochs both in the control window and the silence

485 window into the frequency domain, using an FFT with the same parameters as described above.  
486 Subsequently, we extracted the single phase value associated with the FFT for each epoch and  
487 computed phase coherence as the length of the mean phase vector (Cohen, 2014), for each  
488 participant, condition, frequency, and electrode. While the power for each condition and  
489 frequency was thus computed taking the average over all epochs (e.g., the evoked signal), the  
490 phase consistency was computed on single trial data. We used cluster-based permutation tests  
491 to compare the phase consistency between conditions, with parameters identical to the analysis  
492 of power.

493 **Multiscale entropy (MSE).** MSE is a measure of signal irregularity. To compute MSE,  
494 the EEG signal is divided into patterns of a certain length, and throughout the signal, the number  
495 of repeating patterns is counted. More repetitions indicate a more regular signal, and yield a  
496 lower entropy value. By calculating entropy for patterns of different lengths (“multiscale”), the  
497 contributions of slower and faster timescales in the signal can be assessed. However, the  
498 mapping between entropy timescales and spectral frequencies is not absolute, especially since  
499 entropy is not per se related to a signal being oscillatory in nature (Kloosterman, Kosciessa,  
500 Lindenberger, Fahrenfort, & Garrett, 2020; Kosciessa et al., 2020). The advantage of using  
501 MSE is that it does not require filtering of the data, and it does not assume stationarity (e.g., it  
502 can pick up on regularities that are asymmetrical, or that do not have a fixed amplitude or  
503 period). Here, we computed MSE on the control and silence epochs separately.

504 We computed MSE on high-pass filtered data (0.5 Hz). Epochs were extracted identical  
505 to the epochs for the frequency domain analysis. To compute MSE, we used the mMSE toolbox,  
506 a plugin to the Fieldtrip toolbox (Kloosterman et al., 2020), with  $m = 2$  and  $r = 0.5$ , as was  
507 done previously for EEG data (Kloosterman et al., 2020). For details on how MSE is computed,  
508 see the Supplementary Materials. As for the frequency-domain analysis, we used cluster-based  
509 permutation tests to assess statistical significance. For each comparison between conditions, we

510 used paired t-tests comparing each electrode-timescale combination (note that the above  
511 computation of entropy yields one value per condition for each electrode and timescale) to form  
512 clusters.

513 **Multivariate decoding.** Our exploratory decoding approach is based on the assumption  
514 that temporal expectations are always coupled with feature or spatial expectations (e.g., we  
515 cannot predict “when” without also predicting “what”), as suggested by studies showing that  
516 we only use temporal expectations to improve perception if we can also predict the content  
517 (Morillon et al., 2016; Wollman & Morillon, 2018) or location (O'Reilly et al., 2008) of an  
518 upcoming event. Thus, we expected to be able to decode the representation of the expected  
519 sound at expected moments. As the expected moments are different for each condition, this  
520 then allows us to decode in the silence window whether participants were previously listening  
521 to a beat-based, pattern-based, or random sequence.

522 The decoding was conducted on data that was preprocessed in a similar way as for the  
523 MSE analysis, but with epochs extending from -1800 to 2100 ms relative to the onset of the last  
524 sound. Since the decoding is done in a time resolved way (e.g., sample by sample), there is no  
525 need to leave out the response to the ERPs in the analysis. Additionally, the data were resampled  
526 to 32 Hz to increase signal to noise, using shape-preserving piecewise cubic interpolation, as  
527 implemented in the Fieldtrip toolbox (Oostenveld et al., 2011). Using the ADAM toolbox  
528 (Fahrenfort, van Driel, van Gaal, & Olivers, 2018), we applied a classification algorithm to the  
529 preprocessed data for each participant. Using all electrodes, each dataset was split into 10  
530 equally sized subsets, for 10-fold cross-validation of the decoding. For each subset, a linear  
531 discriminant classifier trained on the remaining 9 subsets was tested. Each condition was  
532 decoded against both other conditions (e.g., beat-based vs. pattern-based, beat-based vs.  
533 random, and pattern-based vs. random), creating a temporal generalization matrix of  
534 classification accuracy at each possible combination of training and testing time points (King

535 & Dehaene, 2014). Subsequently, we examined whether we could observe a pattern of recurrent  
536 activity (King & Dehaene, 2014). Classification accuracies averaged over the 10 folds for each  
537 comparison of two conditions for the silence window (300-2100 ms after the onset of the last  
538 sound) were submitted to cluster-based permutation tests to assess whether they exceeded the  
539 chance level of 0.5. Clusters were based on T-tests with a threshold of 0.05 for each training-  
540 testing time point combination, comparing the accuracy to 0.5.

541 The initial decoding analysis yielded large effects that may be task-related (see Results  
542 for an explanation of these results). Therefore, we ran an additional decoding analysis in which  
543 we decoded expected and unexpected positions against each other within each condition.  
544 Details on this additional analysis can be found in the Supplementary Materials.

545 **Musical expertise.** In an exploratory analysis, we assessed the relationship between the  
546 EEG data and musical expertise. We divided participants in two groups, based on a median split  
547 on the GMSI questionnaire scores. For each EEG marker, we extracted the relevant values  
548 indexing beat-based and pattern-based expectations, and we performed a t-test, comparing the  
549 two musical expertise groups. First, for the CNV-like component in the ERP, we extracted  
550 average amplitudes for each condition in the two windows in which the cluster-based analysis  
551 yielded a significant cluster (300-450 ms and 925-1005 ms, see also Figure 5), from central  
552 electrodes (FC1, FCz, FC2, C1, Cz, C2, CP1, CPz, CP2). To index the effects of temporal  
553 expectations, we then followed the subtraction logic we also used in the analysis of the  
554 behavioral results: the effects of beat-based expectations were quantified as the amplitude in  
555 the beat-based condition minus that in the random condition, and the effects of pattern-based  
556 expectations were quantified as the amplitude in the pattern-based condition minus that in the  
557 random condition. Likewise, for the frequency-domain analysis, we extracted the difference in  
558 power at 1.67 Hz between the beat-based and random conditions, and the difference in power  
559 at 2.22 Hz between the pattern-based and random conditions. Here, we used only electrodes  
560 that contributed to the significant cluster we had found in the silence for the frequency-domain

561 analysis. For the MSE, we similarly extracted differences between entropy in the beat-based  
562 and pattern-based conditions when compared to the random condition, using only electrodes  
563 and timescales that contributed to the significant cluster found in the silence for the MSE  
564 analysis. For decoding, we extracted the classification accuracy when decoding expected  
565 against unexpected times for each participant from the beat-based and pattern-based conditions,  
566 and again contrasted those with the random condition (see Supplementary Materials for details  
567 on this decoding analysis).

568 **Code and data availability.** All datafiles, and code used for data acquisition, data  
569 analysis, and figure creation, are available through <https://osf.io/uwny8/>.

570

571

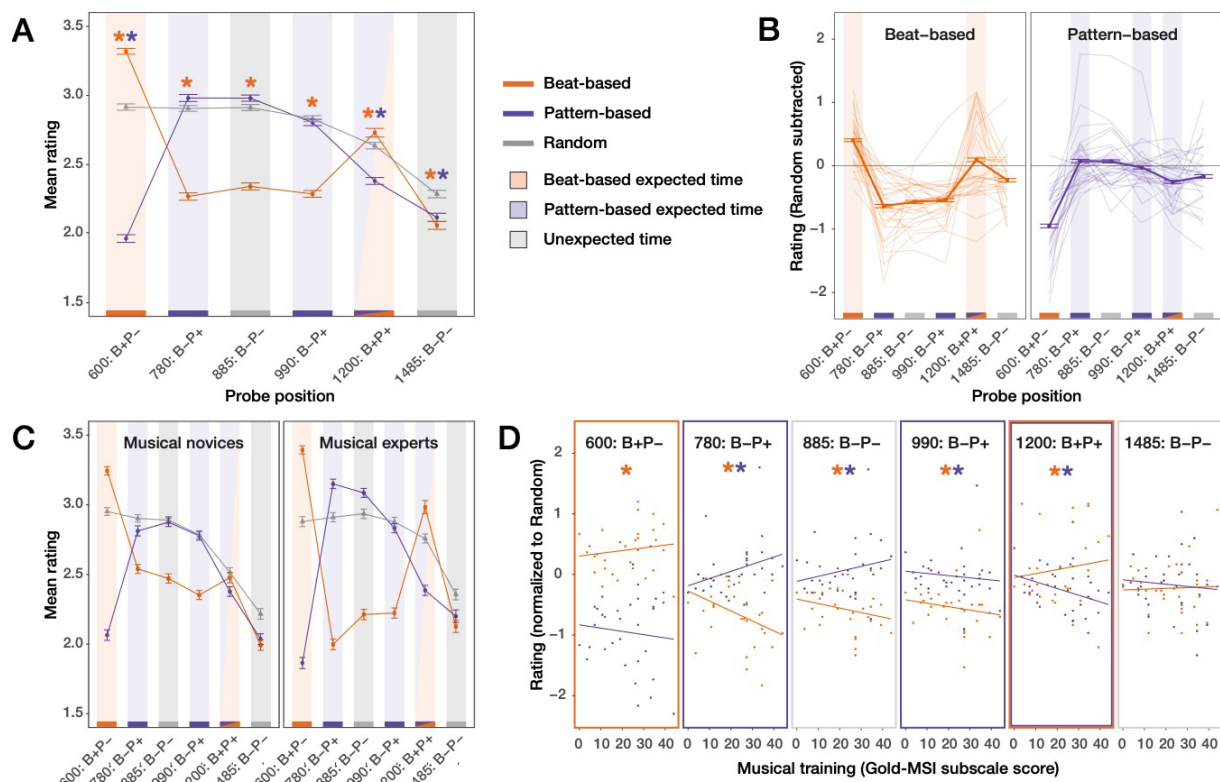
## Results

572 **Behavioral effects of beat-based expectations last multiple beat cycles, while those of**  
573 **pattern-based expectations reflect one interval**

574 Figure 3A shows the average ratings for each condition and probe position from  
575 Experiment 1. Visual inspection of this figure suggests that beat-based expectations were  
576 associated with higher fitness ratings for sounds at expected times than unexpected times for  
577 two beat cycles in the silence window (at 600 and 1200 ms), while the effects of pattern-based  
578 expectations appeared to reflect mainly the first expected time point in the silence window (780  
579 ms). This was confirmed by our statistical analyses. The ordinal regression showed main effects  
580 of Condition ( $\chi^2(2) = 300.72, p < 0.001$ ), Position ( $\chi^2(5) = 1067.05, p < 0.001$ ), as well as  
581 Musical Training ( $\chi^2(1) = 5.16, p = 0.023$ ). However, crucially, these main effects were  
582 accompanied by a very large two-way interaction between Condition and Position ( $\chi^2(10) =$   
583 2478.98,  $p < 0.001$ ), showing that the effects of beat-based and pattern-based expectations on  
584 fitness ratings differed, depending on the position of the probe. We found additional smaller  
585 interactions between Position and Musical Training ( $\chi^2(5) = 67.26, p < 0.001$ ), Condition and  
586 Musical Training ( $\chi^2(2) = 6.01, p = 0.05$ ), and, interestingly, Condition, Position, and Musical  
587 Training ( $\chi^2(10) = 204.88, p < 0.001$ ). Following the interactions, tests of simple main effects  
588 showed that the effect of Position was significant in all conditions (all  $p < 0.001$ ), and the  
589 effect of Condition was significant for all probe positions (all  $p < 0.001$ ). The main effect of  
590 Position in the random condition showed that even after sequences in which no specific  
591 temporal structure was present, ratings depended on the position of the probe. This likely was  
592 due to recency effects. To account for these effects when comparing the ratings at different  
593 positions in the beat-based and pattern-based conditions, we subtracted the ratings in the  
594 random condition at each position from the ratings in the other conditions. The baseline  
595 corrected model (Figure 3B) showed similar interactions between Position and Condition

596  $\chi^2(5) = 2147.55, p < 0.001$ ), and between Position, Condition, and Musical Training ( $\chi^2(5) =$   
 597  $154.46, p < 0.001$ ). The latter indicated that the correlation between Musical Training and the  
 598 rating score depended on both the Position and the Condition of the probe tone.

599



600

601 **Figure 3. The effects of beat-based expectations on fitness ratings can be differentiated from those of**  
 602 **pattern-based expectations, and are associated with musical training.** A) Mean ratings for all conditions  
 603 and positions. Colored asterisks indicate positions where ratings in the beat-based (orange) and pattern-based  
 604 (purple) conditions differed from the random condition at  $p < 0.05$ . B) Single participant data, with the  
 605 random condition subtracted to account for serial position effects. The expectedness pattern is indicated by  
 606 colored lines on the bottom of the plots (orange: expected based on the beat; purple: expected based on  
 607 pattern; grey: neither). For the beat-based condition, ratings followed this pattern for two beat cycles. For the  
 608 pattern-based condition, ratings followed the pattern for one interval. C) Data median split based on scores  
 609 on the musical training questionnaire. The pattern of results, while present for both groups of participants, is  
 610 enhanced for the group of participants with most musical training (“experts”). Note: the median split is for  
 611 visualization purposes only, the models were run with musical training as a covariate. Error bars in panels  
 612 A-C are 2 standard errors (note: these are computed on the complete dataset, not the participant averages, as  
 613 the ordinal model is run on trial-level data). D) Association between musical training and rating for each  
 614 condition and position. Colored asterisks show positions in which the association between musical training  
 615 and the ratings was significantly correlated ( $p < 0.05$ ). A positive association was observed for the beat-based  
 616 condition at 600 and 1200 ms (expected positions) and for the pattern-based condition at 780 (expected) and  
 617 885 ms (unexpected). Negative associations were observed in the beat-based condition at 780, 885, and 990  
 618 ms (all unexpected), and in the pattern-based condition at 990 (unexpected) and 1200 ms (expected).

619

620                   **Beat-based expectations.** At both 600 ms and 1200 ms (expected in terms of a beat),  
621   probes in the beat-based condition were rated as better fitting than probes in the random  
622   condition ( $p < 0.001$  and  $p = 0.004$ ) as evident from the full model; all simple effects from the  
623   full model can be found in Supplementary Table 1). At 780, 885, 990, and 1485 ms (unexpected  
624   in terms of a beat), probes in the beat-condition were rated as worse fitting than probes in the  
625   random condition (all  $ps < 0.001$ ). Moreover, within the beat-based condition, at 600 ms,  
626   baseline corrected ratings were higher than at any other probe position (all  $ps < 0.001$ ), and at  
627   1200 ms baseline corrected ratings were higher than at 780, 885, 990, or 1485 ms (all  $ps <$   
628   0.001). Baseline corrected ratings for probes at 780, 885, and 990 ms (all unexpected in terms  
629   of the beat) did not differ from each (all  $ps > 0.93$ ). Probes at 1485 ms (unexpected in terms of  
630   the beat) were rated as better fitting than probes at 780, 885, and 990 ms (all  $ps < 0.001$ ). All  
631   simple effects from the corrected model can be found in Supplementary Table 2.

632                   As can be seen in Figure 3C and 3D, higher scores on the Musical Training  
633   questionnaire were associated with higher fitness ratings in the beat-based condition at 600 and  
634   1200 ms (expected in terms of the beat), but lower fitness ratings at 780, 885, 990, and 1485  
635   ms (unexpected in terms of the beat). In other words, musically trained participants were better  
636   able to differentiate between probes that were in expected and unexpected positions (Figure  
637   3C). Slopes reach significance at all positions except 1485 ms (all  $ps < 0.022$ ). Also, the  
638   association between Musical Training and ratings differed between beat-based and pattern-  
639   based conditions, at 600, 780, 885, and 1200 ms (all  $ps < 0.004$ ).

640                   To sum up, for the beat-based sequences, we could observe a clear pattern in the results  
641   indicating that beat-based expectations were used to rate the probes well into the silence  
642   window, affecting ratings up to 1200 ms after the onset of the last sound. Beat-based  
643   expectations lead to higher ratings for expected probes (600 and 1200 ms), and lower ratings  
644   for unexpected probes (780, 885, 990, and 1485 ms), both when comparing ratings for each

645 position to the random condition, and when comparing ratings for each position within the beat-  
646 based condition. At 1200 ms, these effects resulted in a classic inverted U-curve, as previously  
647 associated with beat-based processing (Bauer et al., 2015; Jones et al., 2002), with optimal  
648 performance on the beat, and diminished performance on either side (e.g., both earlier and  
649 later). The effects of beat-based expectations did diminish over time, as is apparent from  
650 differences between ratings at 600 and 1200 ms, and at 1485 ms and other unexpected time  
651 points. Both the enhancing and attenuating effects of beat-based expectations were correlated  
652 with musical training. It is worth noting that the longer lasting effects of beat-based expectations  
653 (at 1200 ms) were very heterogenous in our participant pool. Out of 32 participants in  
654 Experiment 1, only 18 showed the inverted U, with higher ratings at 1200 than at 990 and 1485  
655 ms.

656 **Pattern-based expectations.** For pattern-based sequences, ratings at 600 ms  
657 (unexpected based on the pattern) were lower than for the random sequences ( $p < 0.001$ ) and  
658 lower than at any other position (all  $ps < 0.001$ , baseline corrected model), showing that  
659 participants also formed predictions based on the sequences. In line with this, at 780 ms  
660 (expected in terms of the pattern), ratings were numerically higher in the pattern-based  
661 condition than in the random condition, though this difference did not survive the Bonferroni  
662 correction ( $p = 0.058$ ). After this point, ratings did not differ between pattern-based and random  
663 conditions for probes at 885 (unexpected) and 990 (expected) ms, suggesting that the responses  
664 followed the rhythmic pattern mainly in the beginning of the silent period. In line with this, in  
665 the remainder of the silence window, the ratings continued to deviate from what would be  
666 predicted based on the pattern, with lower ratings for the pattern-based than random condition  
667 at 1200 ms (expected;  $p < 0.001$ ). Ratings were also lower for the pattern-based than random  
668 condition at 1485 ms (unexpected,  $p < 0.001$ ), and ratings at 780 ms (expected) did not differ  
669 from ratings at 885 ms (unexpected), while being marginally higher than at 990 (expected,  $p =$

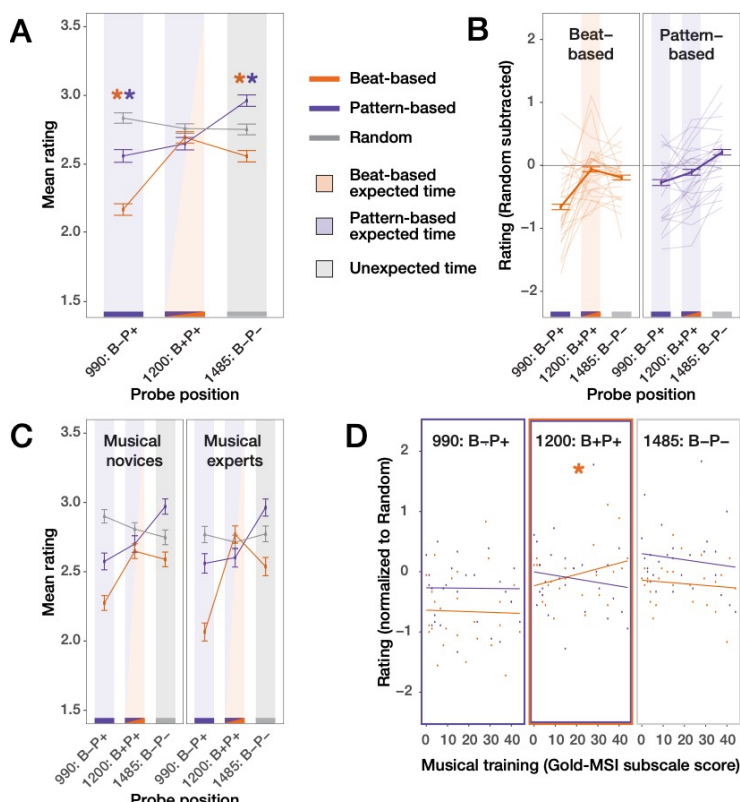
670 0.080), and higher than at 1200 (expected), and 1485 (unexpected) ms (both  $ps < 0.032$ ). In  
671 addition, ratings at 885 and 990 ms were higher than at 1200 and 1485 ms (all  $ps < 0.002$ ). See  
672 Supplementary Tables 1 and 2 for all simple effects.

673 As for beat-based expectations, for pattern-based expectations, there was a positive  
674 association between ratings and musical training at an expected time point (780 ms;  $p < 0.001$ ),  
675 and a negative, albeit nonsignificant, association at an unexpected time point (600 ms). Thus,  
676 like for beat-based expectations, at these early time points, musicians were better able than non-  
677 musicians at differentiating between expected and unexpected moments in time. However, at  
678 885 ms (unexpected in terms of the pattern), the results behaved like at 780 ms, with higher  
679 ratings associated with more Musical Training ( $p = 0.002$ ). At 990 and 1200 ms, Musical  
680 Training was associated with lower ratings (both  $ps < 0.05$ ), but these results are  
681 counterintuitive, as these are expected positions based on the pattern.

682 The results for pattern-based expectations suggest that just like for beat-based  
683 expectations, participants were able to predict the timing of probes based on the preceding  
684 sequence. However, the results show that while this was still the case at 780 ms after the onset  
685 of the last tone, at later probe positions, the effects of pattern-based expectations did not reflect  
686 the preceding sequence. At 885 ms, the results, both in terms of the ratings and how they were  
687 associated with musical training, behaved similar to at 780 ms. After this point, the results  
688 suggest that participants did not use the preceding sequence to guide their responses, but  
689 instead, used a different heuristic.

690 Figure 4 shows the behavioral results obtained from the EEG experiment. Replicating  
691 Experiment 1, we found main effects of Condition ( $\chi^2(2) = 92.30, p < 0.001$ ) and Position  
692 ( $\chi^2(2) = 49.36, p < 0.001$ ), accompanied by interactions between Condition and Position ( $\chi^2(4)$   
693 = 96.62,  $p < 0.001$ ), and Condition, Position, and Musical Training ( $\chi^2(4) = 11.04, p = 0.03$ ).  
694 Following the analysis strategy from Experiment 1, we subtracted the ratings from the Random

695 condition from the ratings for the other two conditions, yielding a baseline corrected model  
696 with similar interactions (Condition and Position:  $\chi^2(2) = 31.46, p < 0.001$ ; Condition, Position,  
697 and Musical Training:  $\chi^2(2) = 8.29, p = 0.02$ ).



698  
699 **Figure 4. Behavioral results during the EEG experiment replicate findings from Experiment 1.** Even  
700 with only 18 trials per participant per condition and position, we could replicate the inverted U-curve for  
701 beat-based sequences at the end of the silence epoch. Like in Experiment 1, the results for the pattern-based  
702 condition do not follow the pattern, but instead, are consistent with building expectations for the next trial.  
703 A) Mean ratings for all conditions and positions. Colored asterisks indicate positions where ratings in the  
704 beat-based (orange) and pattern-based (purple) conditions differed from the random condition (with  $p <$   
705 0.05). B) Single participant data, with the random condition subtracted to account for serial position effects.  
706 C) Data median split based on scores on the musical training questionnaire. Error bars in panels A-C are 2  
707 standard errors. D) Association between musical training and rating for each condition and position. See  
708 Figure 3 for more details.  
709

710 In line with the preceding beat-based sequences, probes at 990 and 1485 ms (both  
711 unexpected times based on the beat) were rated lower in the beat-based condition than in the  
712 random and pattern-based conditions (all  $p < 0.012$ ), and within the beat-based condition,  
713 probes at 1200 ms were rated as better fitting than at 990 ( $p < 0.001$ ) and 1485 ms, though the  
714 latter difference did not reach significance. Thus, like in Experiment 1, we found an inverted  
715 U-curve at 1200 ms after the final tone, suggestive of beat-based expectations lasting at least

716 two beat cycles. As in Experiment 1, at 1200 ms (expected based on the beat), higher ratings in  
717 the beat-based condition were associated with more musical training ( $p = 0.047$ ), suggesting  
718 that the effects of beat-based expectations correlate with musical expertise. Additionally, probes  
719 at 990 ms were rated lower than at 1485 ms ( $p < 0.001$ ), possibly because the effects of beat-  
720 based expectations diminished over the course of the silence.

721 In the pattern-based condition, ratings did not follow the pattern of the preceding  
722 sequences. At 990 ms (expected based on the pattern), probes were rated as worse fitting than  
723 in the random condition ( $p < 0.001$ ), and as worse fitting than at 1200 (expected) and 1485  
724 (unexpected) ms (both  $ps < 0.023$ ), while at 1485 ms (unexpected), probes were rated as better  
725 fitting than in the random condition, and as better fitting than at 1200 (expected) ms (both  $ps <$   
726 0.001). Also, at 1200 ms (expected), higher ratings were associated with less musical training  
727 for the pattern-based condition (though after the Bonferroni correction, only marginally so:  $p =$   
728 0.06), contrary to what would be expected if the effects of expectations are enlarged in musical  
729 experts. All simple effects can be found in Supplementary Tables 1 and 2.

730 Thus, the behavioral results from Experiment 2, though based on less trials than  
731 Experiment 1, suggest a similar pattern as found in Experiment 1: while beat-based expectations  
732 exert their effect well into the silent period, with participant faithfully following the beat in their  
733 goodness-of-fit ratings, pattern-based expectations do not affect ratings in the second half of  
734 the silent period in a manner consistent with the learned pattern. Albeit speculatively, the results  
735 for the pattern-based expectations may be more in line with expectations for the start of the next  
736 trial leading to higher ratings for probe positions closer to the end of the silent period, as in  
737 Experiment 2, after non-probe trials, the next trial followed each silent period at a somewhat  
738 predictable time.

### 739 **Differences in the evoked potential elicited by beat-based and pattern-based sequences**

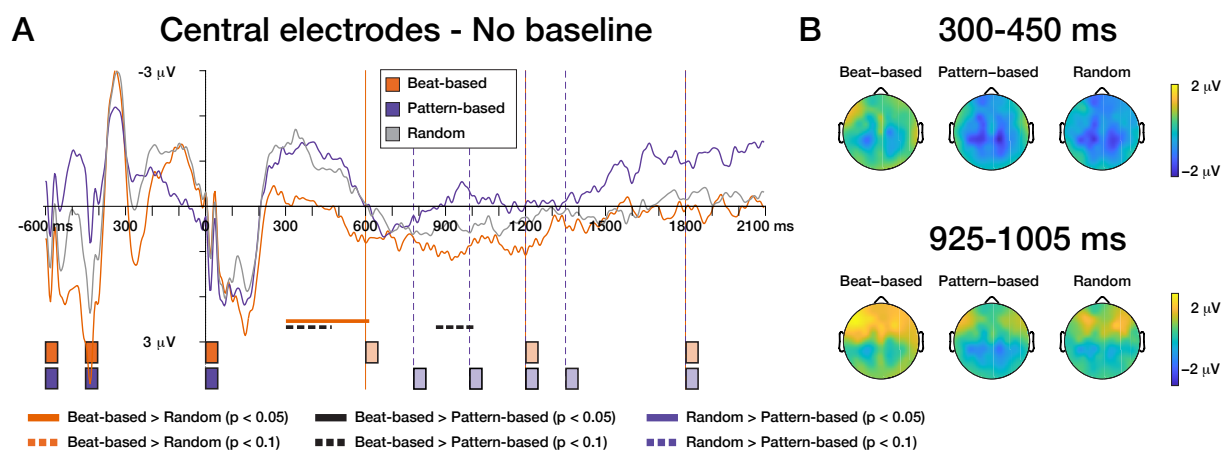
740 Figure 5 shows the average ERPs for each condition, without baseline correction (see  
741 Materials and Methods), and scalp topographies for windows in which we found significant

742 clusters. In line with previous research, we may expect climbing neuronal activity, or a CNV,  
743 flexibly adapting its slope to peak at the moment that participants expect the next event (Breska  
744 & Deouell, 2017; Breska & Ivry, 2020; Damsma, Schlichting, & van Rijn, 2021; Mento, 2013).  
745 We did observe differences in the ERPs between conditions, but the peak of the differences was  
746 not at the expected time, but rather, fell earlier (see Supplementary Figure 1 for the difference  
747 waveforms between conditions). Without baseline correction, the random condition elicited a  
748 significantly more negative ERP ( $p = 0.011$ ) than the beat-based condition in a frontocentral  
749 cluster between 300 and 614 ms after the onset of the last sound (though note that we did not  
750 include timepoints preceding 300 ms in the cluster-based tests). Likewise, in the same latency  
751 range (300 – 473 ms), there was a trend for the pattern-based condition to elicit a more negative  
752 ERP than the beat-based condition ( $p = 0.077$ ). Thus, in a window between approximately 300  
753 and 450 ms, we found tentative evidence for more negative-going waveforms in both the  
754 random and pattern-based condition compared to the beat-based condition, with a central scalp  
755 topography (Figure 5B). In a later window, the pattern-based condition elicited a second  
756 negative deflection, which showed a trend to be larger than in the beat-based condition ( $p =$   
757 0.077, 864 – 1005 ms). While these results were somewhat different depending on the choice  
758 of baseline (see Supplementary Figure 1 for the results with a traditional pre-cue baseline), the  
759 overall picture is the same, with significant clusters in an early and later window indicating  
760 differences between conditions in the ERPs.

761 The time course of the effect deviated from what we expected: the negative deflection  
762 did not peak at the next expected moment in time, but rather, peaked much earlier. Also,  
763 contrary to previous research (Breska & Deouell, 2017), the beat-based condition elicited the  
764 most positive-going ERP, instead of a typical CNV. To further explore and confirm these  
765 results, as a control analysis, we performed the same ERP analysis on the longest time intervals  
766 during the sound presentation. The waveforms showed a negative deflection very similar in

767 morphology and scalp distribution to the one we found in the silence window (see  
768 Supplementary Figure 1). During the sound presentation, like in the silence, this negative  
769 deflection was largest for the pattern-based condition, though the difference was only  
770 significant when comparing the pattern-based condition to the random ( $p = 0.039$ ) but not the  
771 beat-based condition ( $p = 0.1$ ). The latter non-significant result may be due to a noisy baseline,  
772 as during sound presentation, the succession of intervals in the beat-based and random  
773 sequences was (semi-)randomly chosen, and therefore, the baseline was not consistent over  
774 conditions. Overall, however, this control analysis yielded very similar results to the analysis  
775 of ERPs in the silence window.

776 As an exploratory analysis, since musical training was related to larger effects of  
777 entrainment in behavior, we also examined whether there was a relationship between the  
778 amplitude of the negative deflection in the silence window (extracted from the time-electrode  
779 clusters depicted in Figure 5, see Materials and Methods for details) and musical expertise.  
780 However, we found no difference in the effects of expectations on the amplitude of the negative  
781 ERP component between musically trained and untrained subjects (all  $p$ s  $> 0.3$ ).



782 **Figure 5. Beat-based and pattern-based can be differentiated based on ERPs.** A) Left panel show the  
783 grand average waveforms for the silence window for a central electrode cluster (FC1, FCz, FC2, C1, Cz, C2,  
784 CP1, CPz, CP2). Time 0 is the onset of the last tone of the sequence. Colored bars on the bottom of the plots,  
785 and vertical orange and purple lines, indicate at which times a tone would be expected based on the beat  
786 (light orange) and the pattern (light purple). Note that these are expected times, but no sounds were played  
787 during the window shown after time 0. Sounds during the sequence are depicted in dark orange and purple.  
788 B) The scalp distributions for windows in which a significant cluster was observed.

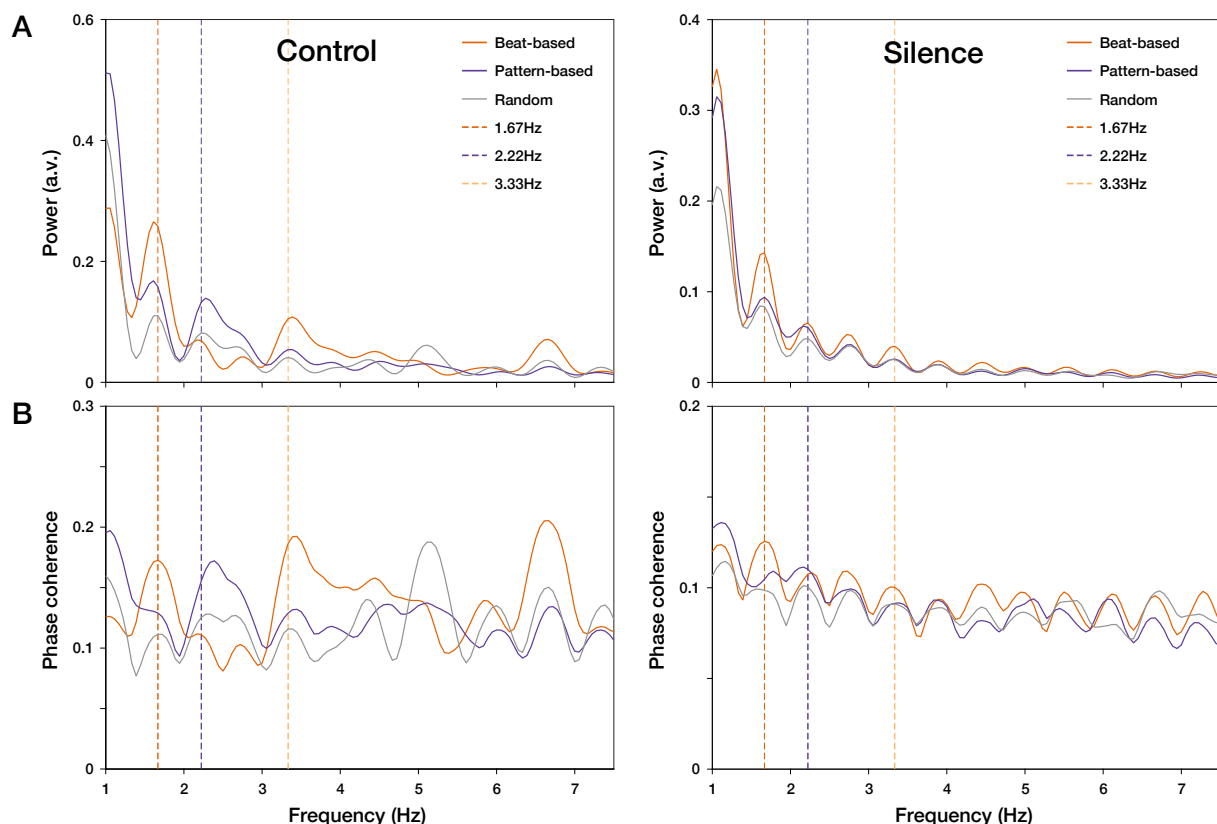
790 **Frequency-domain analysis shows persistent power at the beat frequency following beat-  
791 based sequences**

792 A strong prediction of entrainment theories is that the entrainment outlasts stimulation  
793 with the entraining stimulus. Therefore, we next looked at the frequency content of the EEG  
794 signal in the silent period. Specifically, we predicted that if entrainment occurs, we would find  
795 enhanced power at the frequencies associated with the rhythmic sounds to be found in the  
796 silence. In Figure 6A, the average power for all electrodes, separated for each condition in the  
797 control (i.e. during the auditory sequence) and silence windows is depicted as a function of  
798 frequency. In the control window (Figure 6A, left, and Figure 7, top), the frequency response  
799 followed the sound input. That is, at the beat frequency (1.67 Hz), significant clusters indicated  
800 higher power in the control window for the beat-based sequences than the pattern-based ( $p <$   
801 0.001) and random ( $p = 0.006$ ) sequences. At 2.22 Hz, prominent in the pattern-based and  
802 random sound sequences, higher power was observed in the EEG signal in the pattern-based  
803 than beat-based ( $p = 0.02$ ) and random ( $p = 0.023$ ) sequences, and higher power was observed  
804 in the random than beat-based sequences ( $p = 0.035$ ). Finally, at 3.33 Hz (subdivisions of the  
805 beat), power in the control window was larger for the beat-based than pattern-based ( $p = 0.013$ )  
806 and random ( $p = 0.005$ ) conditions. Thus, in the control window, the EEG signal reflected the  
807 spectral properties of the sound signal, as can be expected, since each sound will have elicited  
808 an ERP, which are represented in steady-state potentials, and thus picked up by the frequency  
809 analysis (Keitel, Obleser, Jessen, & Henry, 2021).

810 Importantly, during the silence (Figure 6A, right, and Figure 7, bottom), no significant  
811 clusters were found at 2.22 Hz, but at the beat frequency (1.67 Hz), power was significantly  
812 larger for the beat-based than the pattern-based ( $p = 0.01$ ) and random ( $p = 0.012$ ) conditions.  
813 In addition, at 3.33 Hz, power for the beat-based condition was larger than for the pattern-based  
814 condition ( $p = 0.038$ ), with a trend when comparing the beat-based with the random condition

815 (p = 0.077). Thus, while the pattern-based and random conditions showed tracking of the sound  
816 during stimulation (which is sometimes considered entrainment “in the broad sense” (Obleser  
817 & Kayser, 2019)), in the silence, entrainment was only present for the beat-based condition.  
818 This finding fits our behavioral observations that beat-based expectations persisted longer in  
819 the silence than pattern-based expectations. To further substantiate the absence of persistent  
820 entrainment at the pattern frequency in the silence, we performed a Bayesian T-test comparing  
821 the normalized power at 2.22 Hz between the pattern-based and random conditions. We found  
822 moderate evidence in favor of the null hypothesis (no difference between conditions) ( $BF_{01} =$   
823 4.5). The results did not change as a function of the prior used (with a more traditional prior of  
824  $r = 1$ ,  $BF_{01} = 6.17$ ).

825 Exploratively, we also compared phase consistency between conditions. Figure 6B  
826 shows the phase consistency averaged over all electrodes for all conditions. In the control  
827 window, there was larger phase consistency at 1.67 and 3.33 Hz in the beat-based than pattern-  
828 based and random conditions (all  $p < 0.001$ ), and larger phase consistency at 2.22 Hz in the  
829 pattern-based than beat-based and random conditions (all  $p < 0.003$ ). In addition, at 2.22 Hz,  
830 phase consistency was higher for the random than beat-based condition ( $p = 0.025$ ). These  
831 results can be expected based on alignment of the evoked potentials in response to the sound.  
832 Crucially, in the silence, phase consistency was larger at 1.67 Hz in the beat-based than random  
833 condition ( $p = 0.025$ ). Neither the difference between the beat-based and pattern-based  
834 condition at 1.67 Hz ( $p = 0.095$ ), nor the difference between the pattern-based and random  
835 condition at 2.22 Hz ( $p = 0.063$ ) reached significance in the cluster-based tests, and none of the  
836 other comparisons yielded any clusters. Thus, this exploratory analysis is in line with the results  
837 obtained from the power analysis. Arguably, this analysis did not yield very strong results, since  
838 phase consistency is also affected by climbing neuronal activity (Breska & Deouell, 2017).



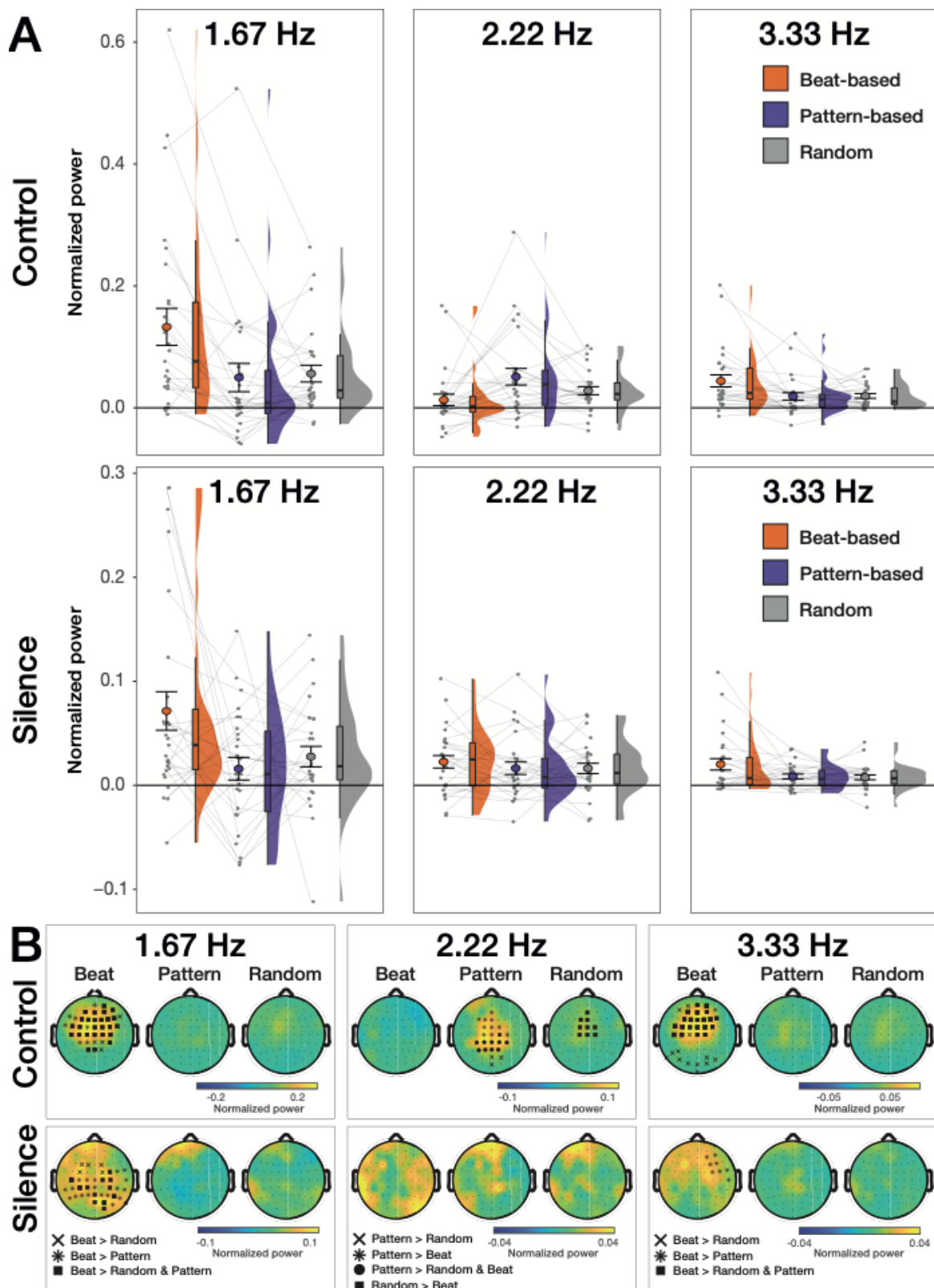
839

840 **Figure 6. Oscillatory power and phase consistency at the beat frequency persist during the silence**  
841 **window.** In the control window, during auditory stimulation, peaks in power (panel A) and phase consistency  
842 (panel B) can be observed at all frequencies of interest, and for the relevant conditions (1.67 and 3.33 Hz in  
843 the beat-based condition, and 2.22 Hz in the pattern-based condition). In the silence window, the peaks in  
844 power at 1.67 and 3.33 Hz were larger in the beat-based condition than in the pattern-based and random  
845 conditions, while peaks at 2.22 Hz did not differ between conditions. The peak in phase coherence at 1.67Hz  
846 in the beat-based condition was larger than in the random condition, while the peak at 2.22 Hz did not differ  
847 between conditions. This suggests that only beat-based expectations persisted in the silence window. Note:  
848 the raw data is depicted here, before the normalization procedure. Data shown is averaged over all electrodes.

849

850 Note that like for the behavioral results indicative of entrainment, there was large  
851 heterogeneity between participants (see Figure 7). While the power differences were significant  
852 in the overall cluster-based analyses, out of 27 participants, only 16 showed on average (i.e.  
853 over all electrodes) numerically larger power in the beat-based condition at the beat frequency  
854 when compared to both the random and pattern-based condition. As for the ERP differences,  
855 musical training did not affect the difference in power between the beat-based and random  
856 condition at 1.67 Hz, nor the difference in power between the pattern-based and random  
857 condition at 2.22 Hz (both  $p > 0.54$ ).

858



859  
860  
861  
862  
863  
864  
865  
866  
867

**Figure 7. Individual participant data shows heterogeneity of the effects of temporal expectations on spectral power.** All plots depict the spectral power at the frequency of interest, averaged over all electrodes, and normalized to account for the 1/f distribution (see Materials and Methods). A) Single participant data, with all data points in grey. Boxplots show the median, with the lower and upper hinges corresponding to the first and third quartiles (25<sup>th</sup> and 75<sup>th</sup> percentiles), and the whiskers corresponding to values no further than 1.5 times the inter-quartile range from the hinges. Error bars depict 2 standard errors around the mean. B) Scalp topographies for all conditions. Electrodes contributing to significant clusters in the cluster-based tests are highlighted on the plots for the conditions in which power was largest.

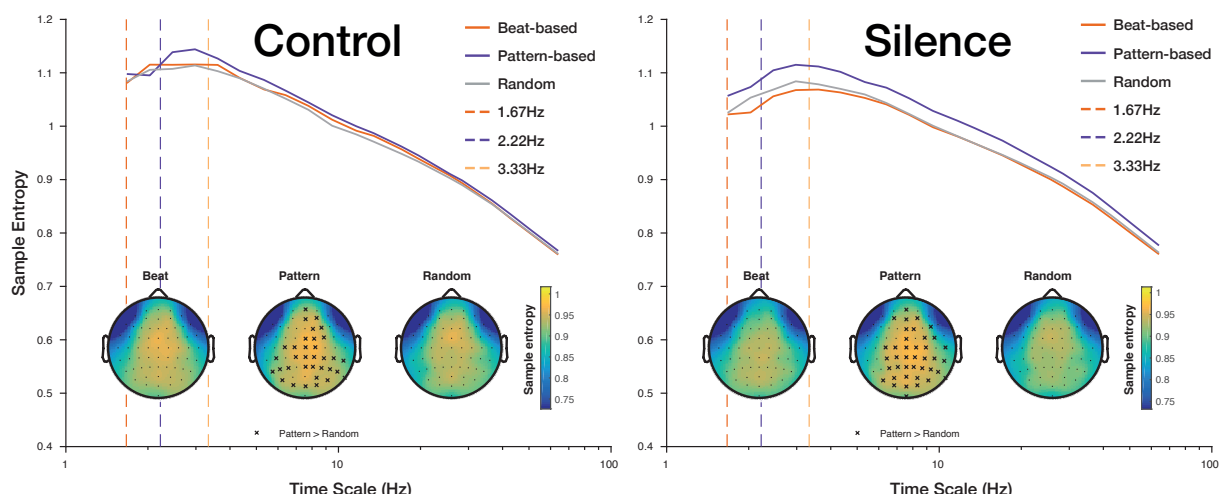
868 **Multiscale entropy as a non-stationary measure of temporal expectations**

869 Figure 8 shows sample entropy for each condition separately, as well as the electrodes  
870 contributing to significant clusters in the analysis. Given that MSE indexes signal irregularity,  
871 we would expect entropy to be higher for the random and pattern-based conditions than for the  
872 beat-based condition in the silence. A cluster-based test on all electrodes and timescales showed  
873 that both in the control window, and in the silence window, entropy was higher for the pattern-  
874 based than for the random condition (control:  $p = 0.03$ ; silence:  $p = 0.021$ ). Note that in the  
875 silence window, all but the two highest timescales were included in the cluster. In the control  
876 window, the cluster spanned all timescales from 35 till 406 ms (see Materials and Methods for  
877 an explanation of the timescales). These results suggest that the signal was more irregular in  
878 the pattern-based than the random condition, over a broad range of timescales. Neither the beat-  
879 based condition compared to pattern-based nor the beat-based compared to the random  
880 condition reached significant differences in entropy, in either control or silence windows (all  
881  $ps > 0.24$ ).

882 Entropy has been related to various other EEG measures, such as spectral power and  
883 overall differences in signal variability (Kosciessa et al., 2020). To account for these, we ran  
884 several additional analyses. First, to check whether the differences in signal variability may  
885 have been caused by differences in low frequency activity, we repeated the MSE analysis on  
886 high-pass filtered data (Kloosterman et al., 2020), using a 5 Hz high-pass filter. This completely  
887 removed the effects (all  $ps > 0.43$ ), suggesting that the differences between conditions were  
888 caused by low frequency activity in the signal (see Supplementary Figure 2).

889 Second, we checked whether differences in signal variability caused the differences in  
890 entropy, since entropy is calculated relative to the overall signal standard deviation (e.g., a  
891 pattern is considered a match at a lower threshold when overall signal variability is high). As  
892 can be seen in Supplementary Figure 3, the similarity bounds used to compute entropy (derived

893 from the time-domain signal standard deviation) differed between conditions, and this  
894 difference mirrored the differences in entropy, suggesting that at least some of the variance we  
895 observed was due to overall signal variability, and not necessarily signal irregularity. Finally,  
896 musical training did not affect the difference in sample entropy between the beat-based and  
897 random condition, nor the difference in entropy between the pattern-based and random  
898 condition (both  $p > 0.66$ ).

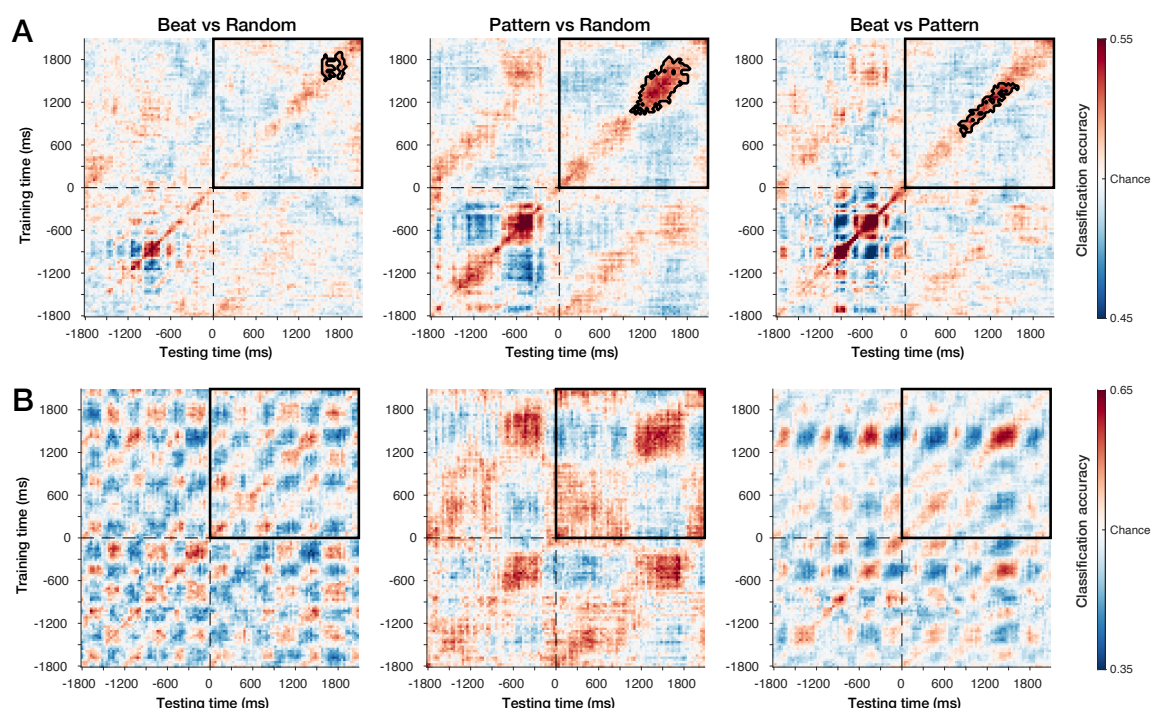


899  
900 **Figure 8. Entropy was higher for pattern-based than random sequences in both control and silence**  
901 **windows.** Entropy in the Control window (left) and Silence window (right), averaged over frontocentral  
902 electrodes, and scalp distributions averaged over all timescales, depicting electrodes contributing to  
903 significant clusters.  
904

## 905 **Multivariate decoding as a time-resolved method for studying entrainment**

906 With multivariate decoding, we expected that training at expected times would yield  
907 above chance performance when testing at expected times, regardless of whether these time  
908 points were the same (e.g., when training at 600 ms, we expected to be able to accurately  
909 distinguish the beat-based from the random condition when testing at not just 600 ms, but also  
910 at 1200 and 1800 ms, as all these times were on the beat, or similarly expected). Figure 9A  
911 shows the temporal generalization matrices for each comparison, with significant clusters  
912 indicated by a black contour. In the silence window we found above chance decoding when  
913 decoding the beat-based against the random condition ( $p = 0.043$ ), the pattern-based against the  
914 random condition ( $p < 0.001$ ), and the beat-based and pattern-based conditions against each

915 other ( $p = 0.009$ ), indicating that based on the EEG signal in the silence, we could classify  
916 which type of rhythm participants had heard just before. However, looking at the temporal  
917 generalization matrices, it becomes apparent that contrary to our expectations, this above-  
918 chance decoding was not due to recurrent activity for expected events. Only clusters on the  
919 diagonal were significant for each comparison. In addition, decoding for all three comparisons  
920 was best in the second halve of the silence window, which is where the probe tones were  
921 presented. This suggests that the decoding mainly picked up on task-related differences. While  
922 the probes were physically identical across conditions, participants may have had different  
923 strategies to perform the task, depending on the type of sequence, and this could have resulted  
924 in above-chance decoding related to the task and probes, even when only analyzing the silence  
925 window.



926  
927 **Figure 9. No recurrent activation in group average decoding, example of recurrency in single**  
928 **participant.** A) Temporal generalization matrices for each comparison for the group analysis. The Y-axis  
929 shows the training time points, and the X-axis testing time points. The color scale indicates the classification  
930 accuracy, with 0.5 being chance level (all analyses are based on decoding two conditions against each other).  
931 Significance of classification accuracy was assessed by using cluster-based permutation tests on the silence  
932 window (300-2100 ms after the last note onset). The black contour indicates significant clusters. Note that  
933 the upper right quadrant, highlighted by the black box, is the entire silence window. B) Temporal  
934 generalization matrix for a participant showing recurrent activity following the expected beats. When  
935 decoding the beat-based vs. the other two conditions (left- and rightmost plots), peaks in accuracy follow a  
936 clear oscillatory pattern, with a phase consistent with the beat-based sequence (600 ms between beats and  
937 decoding peaks).

938 Of note, the decoding results varied considerably between participants. In one  
939 participant in particular (Figure 9B), we observed a pattern in the temporal generalization  
940 matrix that was consistent with the hypothesized result for an oscillatory process (King &  
941 Dehaene, 2014). However, even though some other participants also showed recurrent activity,  
942 the exact times of most accurate decoding, and the exact period of the recurrent process, differed  
943 widely between participants, obscuring these effects in the grand averages. These individual  
944 differences may be caused by individual preferences for a level of regularity in the beat-based  
945 stimuli (Drake, Jones, & Baruch, 2000), with some people attending mostly to the beat level  
946 (1.67 Hz), but others possibly attending to subdivisions (3.33 Hz) or the level of the meter (0.83  
947 Hz). Also, for different people, the optimal phase of delta oscillations (i.e., the phase that aligns  
948 with expected moments) may differ (Breska & Deouell, 2017; Henry & Obleser, 2012),  
949 possibly causing optimal decoding at different time points. To circumvent the large task-related  
950 effects apparent in the decoding results, and the possible individual differences in phase and  
951 metrical level attended to, we ran an additional exploratory decoding analysis looking at  
952 decoding within instead of between conditions. Here, we found above-chance decoding of beat  
953 positions against offbeat positions only following the beat-based condition. However, while  
954 decoding was above chance in the beat-based condition, it was in fact not better than in the  
955 other conditions. As such, these results provide only weak support for persistent effects of beat-  
956 based, but not pattern-based expectations. Detailed results of the within-condition decoding  
957 analysis can be found in the Supplementary Materials (Supplementary Figure 4).

958

959

## Discussion

960 In the current study, we aimed to identify and directly compare the neural mechanisms  
961 underlying temporal expectations based on a regular beat, as well as temporal expectations  
962 based on learning a predictable pattern, by examining the development of climbing activity and  
963 the persistence of neural entrainment after cessation of rhythmic input with either a regular beat,  
964 a predictable pattern of temporal intervals, or random timing. Instead of relying on isochrony  
965 to elicit beat-based expectations, which can also elicit different forms of memory-based  
966 expectations, we used varying non-isochronous patterns to clearly separate beat-based and  
967 pattern-based expectations. Moreover, we assessed responses in a silent period after the  
968 auditory input ceased, side stepping the many possible confounds associated with acoustic  
969 differences between conditions (Capilla, Pazo-Alvarez, Darriba, Campo, & Gross, 2011;  
970 Haegens & Zion Golumbic, 2018; Novembre & Iannetti, 2018; Zoefel et al., 2018).

971 We found several indicators of separate mechanisms for beat-based and pattern-based  
972 expectations. First, behaviorally, we found that while the effects of beat-based expectations  
973 spanned at least two beat cycles, the effects of pattern-based expectations only reflected the  
974 first expected moment in time. Second, a negative ERP component at around 300 to 450 ms  
975 after the onset of the last sound was larger for pattern-based, and possibly random, than beat-  
976 based sequences. Third, we observed significantly more power at the beat frequency in the  
977 silence window when participants were previously listening to a beat-based sequence as  
978 compared to a pattern-based or random sequence, tentatively accompanied by significantly  
979 more phase coherence at the beat frequency in the beat-based condition compared to the random  
980 condition. The observed difference between the behavioral effects of beat-based and pattern-  
981 based expectations and increased oscillatory power at the beat frequency following beat-based  
982 but not pattern-based sequences both point towards entrainment underlying beat-based, but not  
983 pattern-based expectations. The time-domain results showing differences in ERP components

984 between pattern-based and beat-based sequences suggest that the former may rely on a different  
985 mechanism, tentatively more like climbing neuronal activity. Together, these findings provide  
986 support for the notion that beat-based and pattern-based expectations rely on different neural  
987 mechanisms, as has previously been suggested for cue-based expectations (Breska & Deouell,  
988 2017; Breska & Ivry, 2020), but our results do not support models that assume shared  
989 mechanisms, be it entrainment (Tichko & Large, 2019), or a general top-down mechanism for  
990 temporal expectations (Rimmele et al., 2018).

991         Behaviorally, for the beat-based condition, we observed a pattern clearly in line with  
992 entrainment models, with an inverted U-curve, an indication of entrainment (Bauer et al., 2015;  
993 Jones et al., 2002), present as late as 1200 ms after the final tone of each sequence in both  
994 experiments. Beat-based expectations thus affected the fitness ratings for at least two beat  
995 cycles after the end of the sequences, as predicted by nonlinear oscillator models, that assume  
996 oscillations are self-sustaining (Large, 2008; Large & Palmer, 2002). Expectations in the beat-  
997 based condition not only led to higher ratings for expected events, but also to lower ratings for  
998 unexpected events, when compared to the random and pattern-based conditions. Suppression  
999 of unexpected events may be metabolically beneficial (van Atteveldt et al., 2015), and as such,  
1000 has been suggested to be a hallmark of entrainment and the associated “rhythmic” mode of  
1001 processing (Schroeder & Lakatos, 2009a; Zoefel & Vanrullen, 2017). Indeed, suppression off  
1002 the beat has even been proposed to be a better indication of beat-based expectations than  
1003 facilitation on the beat (Bouwer et al., 2020; Breska & Deouell, 2017), in line with the current  
1004 results, where the effects of beat-based expectations at unexpected time points exceeded those  
1005 at expected time points.

1006         Pattern-based expectations similarly affected fitness ratings, with enhanced ratings at  
1007 the first expected time point, and lower ratings at the first unexpected time point, showing that  
1008 participants did form expectations based on the predictable pattern. However, importantly, for

1009 the pattern-based condition, the results are qualitatively different from those for the beat-based  
1010 condition, as the effects of expectations only reflected the first expected moment, but not the  
1011 subsequent structure of the pattern. We did observe lower ratings for the last probe positions  
1012 after pattern-based than random sequences in Experiment 1. One speculative explanation for  
1013 this is that while listeners are able to form expectations following temporal patterns, they only  
1014 do so one interval at a time (e.g., they use each event as a cue for the next interval, but in the  
1015 absence of an event, no next interval is predicted), and in a probabilistic way (Cannon, 2021;  
1016 Damsma et al., 2021; van der Weij, Pearce, & Honing, 2017). In this case, it is possible that the  
1017 expectation for an event at 780 ms would lead to an inverted U-shape in responses, similar to  
1018 the inverted U around a beat, but with a wider distribution. This could explain the ratings being  
1019 equal for probes at 780 and 885 ms, as they would still fall within the time window where a  
1020 tone could be expected, while probes at 1200 and 1485 ms were considered as unexpected, as  
1021 they fell far from the expected time. A tentative alternative explanation could also be that the  
1022 repetitiveness of the pattern lead participants to use a different heuristic during the pattern-  
1023 based sequences to guide their ratings, considering only one interval at a time, while the varying  
1024 rhythmic pattern of the beat-based condition induced a strategy whereby participants were more  
1025 inclined to consider positions after the first expected tone.

1026 Crucial to entrainment models of beat-based expectations (Haegens & Zion Golumbic,  
1027 2018; Henry & Herrmann, 2014; Large, 2008; Large & Jones, 1999; Obleser & Kayser, 2019),  
1028 we found that power at the beat frequency (1.67 Hz) and its harmonic (3.33 Hz) in the EEG  
1029 signal during the silence window was larger following beat-based than pattern-based or random  
1030 sequences. Such enhanced power was not found for a frequency inherent to the pattern-based  
1031 sequence (2.22 Hz). Methodologically, measuring phase locking during rhythmic stimulation  
1032 can lead to confounding contributions from tone-evoked responses (Capilla et al., 2011;  
1033 Novembre & Iannetti, 2018; Zoefel et al., 2018). Ongoing oscillations in silence, after sensory

1034 input has stopped, are therefore regarded as strong evidence for entrainment (Breska & Deouell,  
1035 2017; Haegens & Zion Golumbic, 2018; Obleser & Kayser, 2019; van Bree et al., 2021; Zoefel  
1036 et al., 2018). As such, our observation of enhanced power at the beat frequency during silence  
1037 provides important novel support for the notion that entrainment of low-frequency neural  
1038 oscillations underlies beat-based perception, and our design, using non-isochronous rhythms,  
1039 allows us to separate beat-based aspects from other structure present in natural rhythm (Bouwer,  
1040 Nityananda, Rouse, & ten Cate, 2021).

1041 Interestingly, a recent paper that assessed ongoing oscillations following auditory  
1042 rhythmic input did not find any evidence for persistent entrainment at the frequency of the  
1043 rhythm (Pesnot Lerousseau et al., 2021). Two differences between this study and our work may  
1044 provide directions for future work. First, as mentioned before, isochronous rhythm allows for  
1045 several different ways of forming temporal expectations, including not only beat-based, but  
1046 also cue-based and pattern-based expectations. In the current study, this was the motivation to  
1047 design stimuli that allowed for differentiating between these types of expectations. However,  
1048 an additional concern could be that when presented with stimuli that do not require beat-based  
1049 expectations to perform the task of tracking the temporal structure, the brain may not engage in  
1050 forming such expectations. Thus, in addition to variation between individuals (Assaneo et al.,  
1051 2019), variation in the input signal may also determine which mechanism is used to form  
1052 temporal expectations.

1053 Second, the presence of persistent entrainment may also depend on task demands  
1054 (Shalev, Nobre, & van Ede, 2019). In our study, the auditory sequences were task relevant, and  
1055 the task itself was rhythm-related. In the study by Pesnot Lerousseau et al. (2021), participants  
1056 listened to rhythms passively. This raises the possibility that persistent entrainment is the result  
1057 of explicit, top-down guided expectations, rather than being the result of some passive,  
1058 automatic process (Bouwer, 2022). Interestingly, in our study, the scalp topographies for power

1059 at 1.67 Hz differed between the silence and control windows, with power in the control window  
1060 largest above a frontocentral region, and in the silence window above a parieto-central region.  
1061 This raises the question to what extent the phase locking as measured during the sound  
1062 presentation has the same source as phase locking during the silence. During sound  
1063 presentation, oscillations picked up at the scalp likely contain large contributions from evoked  
1064 responses in auditory cortex that are phase locked to the input (“entrainment in the broad sense”,  
1065 see (Obleser & Kayser, 2019). Possibly, instead of resulting from a sustained automatic  
1066 oscillation, persistent entrainment could originate from other sources, such as explicit  
1067 predictions made by a motor network (Rimmele et al., 2018). The influence of contextual  
1068 factors on entrainment, be it person, stimulus, or task, and the source of phase-locked activity,  
1069 be it automatic phase alignment in sensory cortices, or active top-down expectations, are  
1070 important topics for future research.

1071 The absence of power at 2.22 Hz following the pattern-based sequences suggests that  
1072 entrainment does not underlie expectations based on learning a pattern, contrary to a recently  
1073 proposed oscillator model that can capture aspects of pattern-based expectations (Tichko &  
1074 Large, 2019). In the time-domain, we found a negative deflection in the silence window  
1075 following the pattern-based and random sequences, but less so following the beat-based  
1076 sequences. The observed differences in the ERP suggest that rather than one entrainment  
1077 mechanism for both regular and irregular rhythms, an alternative mechanism, possibly based  
1078 on climbing neuronal activity, specifically supports formation of pattern-based expectations.

1079 The ERP component we observed in the silence window differed from previous work  
1080 and our hypotheses in two respects. First, while previous studies showed a CNV peaking at an  
1081 expected time (Breska & Deouell, 2017; Mento, 2017; Praamstra et al., 2006), here, the peak  
1082 latency of the negative deflection in the signal was earlier, peaking around 400 ms for the  
1083 pattern-based condition, while the first expected time point in the silence was at 780 ms.

1084 Second, in previous research, a CNV was found peaking at expected times not only for cue-  
1085 based, but also for beat-based expectations when compared to a random condition (Breska &  
1086 Deouell, 2012, 2017; Breska & Ivry, 2020; Praamstra et al., 2006). Given the differences  
1087 between our study and previous work looking at the CNV, the question is to what extent the  
1088 negative component we observed in the current study is related to the CNV. Tentatively, we  
1089 would like to suggest that the negative deflection in the current experiment may still be  
1090 interpreted as a CNV, and that differences with previous work may be explained by considering  
1091 the design of the rhythmic stimuli.

1092 First, the CNV may index temporal expectations in a probabilistic, and context-  
1093 dependent way (Capizzi, Correa, & Sanabria, 2013; Damsma et al., 2021; Los & Heslenfeld,  
1094 2005). While the design of most studies looking at the CNV involves isochronous stimulation  
1095 (Breska & Deouell, 2017; Mento, 2017; Praamstra et al., 2006), here, the pattern-based  
1096 sequences contained several temporal intervals with durations between 150 and 780 ms. The  
1097 peak at 400 ms may have indexed the average interval presented in the sequence (~360 ms).  
1098 This explanation is supported by the presence of a deflection with a similar time course and  
1099 morphology for the random condition. Like in the pattern-based condition, in the random  
1100 condition, participants could not use a beat-based strategy to perform the task. Thus, they may  
1101 have attempted to predict the timing of an upcoming sound based on the distribution of the  
1102 absolute intervals, which while random in terms of transitional probabilities, was on average  
1103 identical to the pattern-based condition. Interestingly, the average interval in the beat-based  
1104 condition was also 360 ms, but here, the same component was less present, suggesting that in  
1105 the presence of a possible beat-based strategy, the brain may operate in a rhythmic mode of  
1106 processing (Rimmele et al., 2018; Schroeder & Lakatos, 2009a). Of note, the CNV has indeed  
1107 been shown to be susceptible to its probabilistic context (Capizzi, Correa, & Sanabria, 2013;  
1108 Damsma et al., 2021; Los & Heslenfeld, 2005), and probabilistic models incorporating

1109 statistical regularities in inter-onset intervals at different levels have been used to explain  
1110 aspects of temporal processing (Cannon, 2021; Elliott, Wing, & Welchman, 2014; van der Weij  
1111 et al., 2017). In future work, linking such models directly to neural markers of pattern-based  
1112 expectations may provide more insight in the mechanisms underlying pattern-based  
1113 expectations and how they relate to the CNV.

1114 Secondly, studies finding a CNV for beat-based expectations have typically also used  
1115 isochronous stimulation. Therefore, memory-based expectations, be it pattern-based or cue-  
1116 based, could also have been formed in response to these sequences (Bouwer et al., 2020, 2021;  
1117 Bouwer, Werner, Knetemann, & Honing, 2016; Breska & Ivry, 2016; Keele et al., 1989), and  
1118 may have contributed to the elicitation of a CNV. Here, using a beat-based sequence that did  
1119 not allow for expectations based on simply learning transitional probabilities, we did not  
1120 observe the same negative deflection as in the pattern-based sequences. This raises the  
1121 possibility that a CNV (or CNV-like) component is specific to pattern-based and cue-based  
1122 (Mento, 2013, 2017), temporal expectations.

1123 It could also be argued that the differences we observed in ERPs should not be  
1124 interpreted as a CNV, but rather, were caused by differences in the P3 response to the last sound  
1125 of each sequence, which would be apparent at a similar latency (peaking between 300 and 450  
1126 ms). This would mean that the P3 response would have been largest for expected sounds in the  
1127 beat-based sequences, smallest for expected sounds in the pattern-based sequences, with the  
1128 response to unexpected sounds in the random sequences in between. The P3 has indeed been  
1129 shown to be susceptible to temporal expectations, with larger amplitude responses for  
1130 temporally predictable targets (Lange, 2009; Mento, 2017; Schmidt-Kassow, Schubotz, &  
1131 Kotz, 2009). However, these effects can be observed for beat-based and memory-based  
1132 expectations in a similar direction (Breska & Deouell, 2017; Breska & Ivry, 2020; Mento, 2017;  
1133 Schmidt-Kassow et al., 2009). Thus, we feel it is unlikely that the differences observed in the

1134 ERPs here are caused by differences in the P3, as the P3, if anything, should have been larger  
1135 for the pattern-based than random sequences, which is not the case. Thus, we tentatively suggest  
1136 that here, the observed ERP differences are more likely to be due to a CNV-like mechanism.

1137 Various other challenges for future research remain. First, in the beat-based condition,  
1138 it could be argued that participants used an interval-based strategy to perform the task, in which  
1139 they predicted an event every 600 ms. However, listening to strictly metric patterns, as the ones  
1140 used here, is associated with activity in a circuit including the basal ganglia, while listening to  
1141 non-metric patterns is associated with activity in a circuit including the cerebellum, making it  
1142 unlikely that the same, interval-based mechanism would be used for both types of rhythms  
1143 (Leow & Grahn, 2014). Also, predicting the timing of events in non-isochronous strictly metric  
1144 sequences would require participants to learn not just the transitional probabilities of single  
1145 intervals, but also to combine multiple intervals into groups that together last the length of a  
1146 beat. It is currently unclear whether humans, when faced with rhythmic patterns, use such a  
1147 hierarchical interval-based strategy. Indeed, future research could examine if beat-based  
1148 expectations in general can be explained by such multilevel interval learning, akin to a recent  
1149 model for beat-based perception (Cannon & Patel, 2021), as this could provide a general  
1150 challenge to oscillator models of beat-based perception. In such a view, the difference between  
1151 beat-based and pattern-based timing may be the importance of hierarchical structure in beat-  
1152 based rhythms (Fitch, 2013), rather than the presence of oscillations.

1153 A second challenge concerns the result from the frequency-domain analysis. The  
1154 Fourier transform assumes stationarity in the oscillating signal, while entrainment models  
1155 propose a dampening factor to account for decreasing oscillatory power over time (Large,  
1156 Herrera, & Velasco, 2015). To assess power at specific frequencies in a time-resolved way,  
1157 wavelet convolution is often used as an alternative. But, in the current study, differentiating  
1158 between the specific frequencies of the beat and the pattern would require wavelet parameters

1159 that would result in a temporal resolution too low to disentangle activity during and before the  
1160 silence (i.e., many wavelet cycles would be needed). Recently, a promising alternative to assess  
1161 oscillatory activity in the time domain was proposed in the form of cycle-by-cycle analysis  
1162 (Cole & Voytek, 2019). However, this approach requires filtering the signal at the specific  
1163 frequency of interest, again posing problems for disentangling low frequency oscillations due  
1164 to the beat, the pattern, and ongoing ERPs. Assessing the time course of low frequency  
1165 oscillations thus remains a challenge for future research.

1166 Multi scale entropy and multivariate pattern analysis may provide alternative ways to  
1167 examine neural entrainment with high temporal precision. At the group level, entropy was  
1168 higher following the pattern-based than random sequences. This could be explained by  
1169 assuming that the brain uses a vigilance mode to track the pattern-based regularities, which at  
1170 the neural level, translates in more irregular patterns of activity. Attention and arousal, which  
1171 are both associated with temporal expectations (Schroeder & Lakatos, 2009b), have indeed  
1172 been linked to neural variability as well (Waschke et al., 2021). However, the group level results  
1173 can be explained at least to some extent by overall differences in signal variability (e.g., the  
1174 signal variance), so this hypothesis remains to be confirmed in future research. Considering the  
1175 decoding results, the observed above-chance decoding seemed to primarily reflect general task-  
1176 related activity. The best decoding was observed in the second half of the silence window,  
1177 where probes could be presented. Also, in the group-average decoding results, above chance  
1178 decoding was limited to training and testing on the same time points. In other words, we did  
1179 not observe recurrent activity, as reflected in stronger decoding accuracy at expected time  
1180 points. Yet, we did show a proof of concept for our approach in at least one participant, who  
1181 showed a clear oscillatory pattern in decoding accuracy when decoding the beat-based against  
1182 the other two conditions. This pattern of activity is in line with the strength or sharpness of the

1183 neural representation of tones varying over time as a function of temporal expectations  
1184 (Auksztulewicz et al., 2019, 2018).

1185 At the group level, the behavioral results, along with the results obtained using  
1186 frequency-domain analysis and ERPs provide evidence for differential processing of the beat  
1187 and the pattern in rhythm, while the results from the decoding and entropy analyses are less  
1188 clear. One reason for this is heterogeneity between individuals. This heterogeneity may be  
1189 present at several levels. First, people may attend to different levels of regularity in beat-based  
1190 perception (Drake et al., 2000), and the optimal phase of delta oscillations (e.g., the phase that  
1191 aligns with expected moments) may differ across individuals (Breska & Deouell, 2017; Henry  
1192 & Obleser, 2012; Sun et al., 2021). Second, while it is often assumed that most people  
1193 automatically form beat-based expectations (Honing, 2012), recent evidence showed phase  
1194 locking to speech in only about half of the population (Assaneo et al., 2019). Indeed, in our  
1195 study, only about two-thirds of the participants behaviorally showed evidence for beat-based  
1196 expectations in the second half of the silence window and we only observed enhanced power  
1197 at the beat frequency following beat-based sequences in about half of the participants.

1198 In the current study, the behavioral effects of beat-based and pattern-based expectations  
1199 were associated with musical training, consistent with previous research using beat-based  
1200 (Bouwer et al., 2018, 2016; Cameron & Grahn, 2014; Matthews, Thibodeau, Gunther, &  
1201 Penhune, 2016; Vuust et al., 2005) and pattern-based (Cameron & Grahn, 2014) rhythms. Some  
1202 previous studies have failed to show differences between musicians and non-musicians,  
1203 however (Bouwer, Van Zuijen, & Honing, 2014; Geiser et al., 2009; Grahn & Brett, 2007),  
1204 possibly due to differences in task design (Bouwer et al., 2018). The current study used an  
1205 explicit rating task, for which performance may be particularly improved by musical training,  
1206 as musically trained participants may have additional strategies to perform the task. The use of  
1207 implicit timing tasks may be a better probe of innate differences in timing abilities, which need

1208 not necessarily be related to musical training (Law & Zentner, 2012), and implicit tasks may  
1209 also be less susceptible to task-related effects as we observed in the decoding analysis, which  
1210 may stem from individual strategies in performing the explicit task.

1211 We did not find an association between musical expertise and the neural results. This  
1212 may be due to neural activity being more reflective of innate abilities, as argued above. Also,  
1213 our sample scored relatively low on the musical training scale, with a mean of 20.5 on the GMSI  
1214 subscale, which is comparable to the 32<sup>nd</sup> percentile of the norm scores, which have a mean of  
1215 26.5 (Müllensiefen et al., 2014). This may have made it hard to find the effects of musical  
1216 training. However, with the current sample size, we may have simply lacked power to detect  
1217 associations between neural data and musical expertise. Undoubtedly, given the heterogeneity  
1218 we and others (Assaneo et al., 2019; Bauer et al., 2015; Sun et al., 2021) have observed in tasks  
1219 probing temporal expectations, understanding individual differences is an important direction  
1220 for future research, with significant implications for applications of musical rhythm, such as in  
1221 motor rehabilitation (Dalla Bella, Dotov, Bardy, & Cochen De Cock, 2018).

## 1222 Conclusion

1223 In summary, we have shown that beat-based and pattern-based expectations can be  
1224 differentiated in terms of their behavioral and neurophysiological effects once sensory input  
1225 has ceased. These findings provide novel, more conclusive evidence for the notion that different  
1226 mechanisms implement temporal expectations based on periodic and aperiodic input streams,  
1227 with the former based on entrainment of low frequency neural oscillations, and the latter on  
1228 climbing neural activity indexing a memorized interval.

## 1229 Acknowledgements

1230 We would like to thank Babak Chawoush and Charlotte van Roijen for their assistance  
1231 with the data collection, and fruitful discussions during the project.

1232

1233

## References

1234 Arnal, L. H., Doelling, K. B., & Poeppel, D. (2014). Delta-beta coupled oscillations underlie temporal prediction  
1235 accuracy. *Cerebral Cortex*, 25(9), 3077–3085. <https://doi.org/10.1093/cercor/bhu103>

1236 Assaneo, M. F., Ripollés, P., Orpella, J., Lin, W. M., de Diego-Balaguer, R., & Poeppel, D. (2019). Spontaneous  
1237 synchronization to speech reveals neural mechanisms facilitating language learning. *Nature Neuroscience*,  
1238 22(4), 627–632. <https://doi.org/10.1038/s41593-019-0353-z>

1239 Auksztulewicz, R., Myers, N. E., Schnupp, J. W., & Nobre, A. C. (2019). Rhythmic temporal expectation boosts  
1240 neural activity by increasing neural gain. *The Journal of Neuroscience*, 39(49), 9806–9817.  
1241 <https://doi.org/10.1523/JNEUROSCI.0925-19.2019>

1242 Auksztulewicz, R., Schwiedrzik, C. M., Thesen, T., Doyle, W., Devinsky, O., Nobre, A. C., ... Melloni, L.  
1243 (2018). Not all predictions are equal: “What” and “when” predictions modulate activity in auditory cortex  
1244 through different mechanisms. *The Journal of Neuroscience*, 38(40), 8680–8693.  
1245 <https://doi.org/10.1523/JNEUROSCI.0369-18.2018>

1246 Bauer, A.-K. R., Jaeger, M., Thorne, J. D., Bendixen, A., & Debener, S. (2015). The auditory dynamic attending  
1247 theory revisited: A closer look at the pitch comparison task. *Brain Research*, 1626, 198–210.  
1248 <https://doi.org/10.1016/j.brainres.2015.04.032>

1249 Bouwer, F. L. (2022). Neural entrainment to auditory rhythms: Automatic or top-down driven? *Journal of*  
1250 *Neuroscience*, 42(11), 2146–2148. <https://doi.org/10.1523/JNEUROSCI.2305-21.2022>

1251 Bouwer, F. L., Burgoine, J. A., Odijk, D., Honing, H., & Grahn, J. A. (2018). What makes a rhythm complex?  
1252 The influence of musical training and accent type on beat perception. *PLOS ONE*, 13(1), e0190322.  
1253 <https://doi.org/10.1371/journal.pone.0190322>

1254 Bouwer, F. L., & Honing, H. (2015). Temporal attending and prediction influence the perception of metrical  
1255 rhythm: Evidence from reaction times and ERPs. *Frontiers in Psychology*, 6(July), 1094.  
1256 <https://doi.org/10.3389/fpsyg.2015.01094>

1257 Bouwer, F. L., Honing, H., & Slagter, H. A. (2020). Beat-based and memory-based temporal expectations in  
1258 rhythm: similar perceptual effects, different underlying mechanisms. *Journal of Cognitive Neuroscience*,  
1259 32(7), 1221–1241. [https://doi.org/10.1162/jocn\\_a\\_01529](https://doi.org/10.1162/jocn_a_01529)

1260 Bouwer, F. L., Nityananda, V., Rouse, A. A., & ten Cate, C. (2021). Rhythmic abilities in humans and non-  
1261 human animals: A review and recommendations from a methodological perspective. *Philosophical*  
1262 *Transactions of the Royal Society B*, 376, 20200335. <https://doi.org/10.1098/rstb.2020.0335>

1263 Bouwer, F. L., Van Zuijen, T. L., & Honing, H. (2014). Beat processing is pre-attentive for metrically simple  
1264 rhythms with clear accents: An ERP study. *PLoS ONE*, 9(5), e97467.  
1265 <https://doi.org/10.1371/journal.pone.0097467>

1266 Bouwer, F. L., Werner, C. M., Knetemann, M., & Honing, H. (2016). Disentangling beat perception from  
1267 sequential learning and examining the influence of attention and musical abilities on ERP responses to  
1268 rhythm. *Neuropsychologia*, 85, 80–90. <https://doi.org/10.1016/j.neuropsychologia.2016.02.018>

1269 Breska, A., & Deouell, L. Y. (2012). Automatic bias of temporal expectations following temporally regular input  
1270 independently of high-level temporal expectation. *Journal of Cognitive Neuroscience*, 26(7), 1555–1571.  
1271 <https://doi.org/10.1162/jocn>

1272 Breska, A., & Deouell, L. Y. (2017). Neural mechanisms of rhythm-based temporal prediction: Delta phase-  
1273 locking reflects temporal predictability but not rhythmic entrainment. *PLOS Biology*, 15(2), e2001665.  
1274 <https://doi.org/10.1371/journal.pbio.2001665>

1275 Breska, A., & Ivry, R. B. (2016). Taxonomies of timing: where does the cerebellum fit in? *Current Opinion in*  
1276 *Behavioral Sciences*, 8, 282–288. <https://doi.org/10.1016/J.COBEHA.2016.02.034>

1277 Breska, A., & Ivry, R. B. (2018). Double dissociation of single-interval and rhythmic temporal prediction in  
1278 cerebellar degeneration and Parkinson’s disease. *Proceedings of the National Academy of Sciences*,  
1279 115(48), 12283–12288. <https://doi.org/10.1073/pnas.1810596115>

1280 Breska, A., & Ivry, R. B. (2020). Context-specific control over the neural dynamics of temporal attention by the  
1281 human cerebellum. *Science Advances*, 6(49), 1–16. <https://doi.org/10.1126/sciadv.abb1141>

1282 Brysbaert, M., & Stevens, M. (2018). Power analysis and effect size in mixed effects models: A tutorial. *Journal*  
1283 *of Cognition*, 1(1), 1–20. <https://doi.org/10.5334/joc.10>

1284 Cameron, D. J., & Grahn, J. A. (2014). Enhanced timing abilities in percussionists generalize to rhythms without  
1285 a musical beat. *Frontiers in Human Neuroscience*, 8(December), 1003.  
1286 <https://doi.org/10.3389/fnhum.2014.01003>

1287 Cannon, J. J. (2021). Expectancy-based rhythmic entrainment as continuous Bayesian inference. *PLoS*  
1288 *Computational Biology*, 17(6), e1009025. <https://doi.org/10.1371/journal.pcbi.1009025>

1289 Cannon, J. J., & Patel, A. D. (2021). How Beat Perception Co-opts Motor Neurophysiology. *Trends in Cognitive*  
1290 *Sciences*, 25(2), 137–150. <https://doi.org/10.1016/j.tics.2020.11.002>

1291 Capilla, A., Pazo-Alvarez, P., Darriba, A., Campo, P., & Gross, J. (2011). Steady-State Visual Evoked Potentials

1292 Can Be Explained by Temporal Superposition of Transient Event-Related Responses. *PLoS ONE*, 6, 1293 e14543. <https://doi.org/10.1371/journal.pone.0014543>

1294 Capizzi, M., Correa, Á., & Sanabria, D. (2013). Temporal orienting of attention is interfered by concurrent 1295 working memory updating. *Neuropsychologia*, 51(2), 326–339. 1296 <https://doi.org/10.1016/j.neuropsychologia.2012.10.005>

1297 Carifio, J., & Perla, R. (2008). Resolving the 50-year debate around using and misusing Likert scales. *Medical 1298 Education*, 42(12), 1150–1152. <https://doi.org/10.1111/j.1365-2923.2008.03172.x>

1299 Christensen, R. H. B. (2019). ordinal - Regression models for Ordinal Data. R package version 2019.4-25. 1300 Retrieved from <http://www.cran.r-project.org/package=ordinal/>

1301 Cohen, M. X. (2014). *Analyzing neural time series data: theory and practice*. MIT press.

1302 Cole, S., & Voytek, B. (2019). Cycle-by-cycle analysis of neural oscillations. *Journal of Neurophysiology*, 122, 1303 849–861. <https://doi.org/10.1152/jn.00273.2019>

1304 Cravo, A. M., Rohenkohl, G., Wyart, V., & Nobre, A. C. (2013). Temporal expectation enhances contrast 1305 sensitivity by phase entrainment of low-frequency oscillations in visual cortex. *The Journal of 1306 Neuroscience*, 33(9), 4002–4010. <https://doi.org/10.1523/JNEUROSCI.4675-12.2013>

1307 Dalla Bella, S., Dotov, D., Bardy, B., & Cochen De Cock, V. (2018). Individualization of music-based rhythmic 1308 auditory cueing in Parkinson's disease. *Annals of the New York Academy of Sciences*, 1423, 308–317. 1309 <https://doi.org/10.1111/nyas.13859>

1310 Damsma, A., Schlichting, N., & van Rijn, H. (2021). Temporal context actively shapes EEG signatures of time 1311 perception. *The Journal of Neuroscience*. <https://doi.org/10.1523/JNEUROSCI.0628-20.2021>

1312 de Graaf, T. A., Gross, J., Paterson, G., Rusch, T., Sack, A. T., & Thut, G. (2013). Alpha-Band Rhythms in 1313 Visual Task Performance: Phase-Locking by Rhythmic Sensory Stimulation. *PLoS ONE*, 8(3), e60035. 1314 <https://doi.org/10.1371/journal.pone.0060035>

1315 Delorme, A., & Makeig, S. (2004). EEGLAB: an open source toolbox for analysis of single-trial EEG dynamics 1316 including independent component analysis. *Journal of Neuroscience Methods*, 134, 9–21. 1317 <https://doi.org/10.1016/j.jneumeth.2003.10.009>

1318 Ding, N., Patel, A. D., Chen, L., Butler, H., Luo, C., & Poeppel, D. (2017). Temporal modulations in speech and 1319 music. *Neuroscience and Biobehavioral Reviews*, 81, 181–187. 1320 <https://doi.org/10.1016/j.neubiorev.2017.02.011>

1321 Doelling, K. B., & Assaneo, M. F. (2021). Neural oscillations are a start toward understanding brain activity 1322 rather than the end. *PLoS Biology*, 19(5), 1–12. <https://doi.org/10.1371/journal.pbio.3001234>

1323 Doelling, K. B., Assaneo, M. F., Bevilacqua, D., Pesaran, B., & Poeppel, D. (2019). An oscillator model better 1324 predicts cortical entrainment to music. *Proceedings of the National Academy of Sciences*, 116(20), 10113– 1325 10121. <https://doi.org/10.1073/pnas.1816414116>

1326 Donoghue, T., Schawronkow, N., & Voytek, B. (2021). Methodological considerations for studying neural 1327 oscillations. *European Journal of Neuroscience*, (January), 1–26. <https://doi.org/10.1111/ejn.15361>

1328 Drake, C., Jones, M. R., & Baruch, C. (2000). The development of rhythmic attending in auditory sequences: 1329 attunement, referent period, focal attending. *Cognition*, 77(3), 251–288. [https://doi.org/10.1016/S0010-0277\(00\)00106-2](https://doi.org/10.1016/S0010- 1330 0277(00)00106-2)

1331 Elliott, M. T., Wing, A. M., & Welchman, A. E. (2014). Moving in time: Bayesian causal inference explains 1332 movement coordination to auditory beats. *Proceedings of the Royal Society B*, 281(May), 20140751.

1333 Fahrenfort, J. J., van Driel, J., van Gaal, S., & Olivers, C. N. L. (2018). From ERPs to MVPA Using the 1334 Amsterdam Decoding and Modeling Toolbox (ADAM). *Frontiers in Neuroscience*, 12, 368. 1335 <https://doi.org/10.3389/fnins.2018.00368>

1336 Fitch, W. T. (2013). Rhythmic cognition in humans and animals: distinguishing meter and pulse 1337 perception. *Frontiers in systems neuroscience*, 7, 68. <https://doi.org/10.3389/fnsys.2013.00068>

1338 Fox, J., & Weisberg, S. (2019). *An R Companion to Applied Regression* (3rd ed.). Thousand Oaks (CA): Sage. 1339 Retrieved from <https://socialsciences.mcmaster.ca/jfox/Books/Companion/>

1340 Geiser, E., Ziegler, E., Jancke, L., Meyer, M., Jäncke, L., Meyer, M., ... Meyer, M. (2009). Early 1341 electrophysiological correlates of meter and rhythm processing in music perception. *Cortex*, 45(1), 93– 1342 102. <https://doi.org/10.1016/j.cortex.2007.09.010>

1343 Grahn, J. A., & Brett, M. (2007). Rhythm and beat perception in motor areas of the brain. *Journal of Cognitive 1344 Neuroscience*, 19(5), 893–906. <https://doi.org/10.1162/jocn.2007.19.5.893>

1345 Grahn, J. A., & Rowe, J. B. (2009). Feeling the beat: premotor and striatal interactions in musicians and 1346 nonmusicians during beat perception. *The Journal of Neuroscience*, 29(23), 7540–7548. 1347 <https://doi.org/10.1523/JNEUROSCI.2018-08.2009>

1348 Haegens, S., & Zion Golumbic, E. (2018). Rhythmic facilitation of sensory processing: A critical review. 1349 *Neuroscience and Biobehavioral Reviews*, 86(March), 150–165. 1350 <https://doi.org/10.1016/j.neubiorev.2017.12.002>

1351 Heideman, S. G., van Ede, F., & Nobre, A. C. (2018). Early Behavioural Facilitation by Temporal Expectations

1352 in Complex Visual-motor Sequences. *Neuroscience*, 389, 74–84.  
1353 <https://doi.org/10.1016/J.NEUROSCIENCE.2018.05.014>

1354 Henry, M. J., & Herrmann, B. (2014). Low-frequency neural oscillations support dynamic attending in temporal  
1355 context. *Timing & Time Perception*, 2(1), 62–86. <https://doi.org/10.1163/22134468-00002011>

1356 Henry, M. J., Herrmann, B., & Obleser, J. (2014). Entrained neural oscillations in multiple frequency bands  
1357 comodulate behavior. *Proceedings of the National Academy of Sciences*, 111(41), 14935–14940.  
1358 <https://doi.org/10.1073/pnas.1408741111>

1359 Henry, M. J., & Obleser, J. (2012). Frequency modulation entrains slow neural oscillations and optimizes human  
1360 listening behavior. *Proceedings of the National Academy of Sciences*, 109(49), 20095–20100.  
1361 <https://doi.org/10.1073/pnas.1213390109>

1362 Herbst, S. K., Stefanics, G., & Obleser, J. (2022). Endogenous modulation of delta phase by expectation—A  
1363 replication of Stefanics et al., 2010. *Cortex*, 149, 226–245. <https://doi.org/10.1016/j.cortex.2022.02.001>

1364 Hickok, G., Farahbod, H., & Saberi, K. (2015). The Rhythm of Perception: Entrainment to Acoustic Rhythms  
1365 Induces Subsequent Perceptual Oscillation. *Psychological Science*, 26(7), 1006–1013.  
1366 <https://doi.org/10.1177/0956797615576533>

1367 Honing, H. (2012). Without it no music: beat induction as a fundamental musical trait. *Annals of the New York  
1368 Academy of Sciences*, 1252(1), 85–91. <https://doi.org/10.1111/j.1749-6632.2011.06402.x>

1369 Honing, H., & Bouwer, F. L. (2019). Rhythm. In P. J. Rentfrow & D. Levitin (Eds.), *Foundations in Music  
1370 Psychology: Theory and Research* (pp. 33–69). Cambridge, MA: MIT Press.

1371 Iversen, J. R., & Patel, A. D. (2008). The Beat Alignment Test (BAT): Surveying beat processing abilities in the  
1372 general population. In K. Miyazaki, Y. Hiraga, M. Adachi, Y. Nakajima, & M. Tsuzaki (Eds.), *10th Intl.  
1373 Conf. on Music Perception and Cognition* (pp. 465–468). Adelaide: Causal Productions.

1374 Jamieson, S. (2004). Likert scales: How to (ab)use them. *Medical Education*, 38(12), 1217–1218.  
1375 <https://doi.org/10.1111/j.1365-2929.2004.02012.x>

1376 JASP, T. (2019). JASP. Retrieved from <https://jasp-stats.org>

1377 Jeffreys, H. (1961). *Theory of probability* (3rd ed.). Oxford, UK: Oxford University Press.

1378 Jones, M. R., Moynihan, H., MacKenzie, N., & Puente, J. (2002). Temporal aspects of stimulus-driven attending  
1379 in dynamic arrays. *Psychological Science*, 13(4), 313–319. <https://doi.org/10.1111/1467-9280.00458>

1380 Keele, S. W., Nicoletti, R., Ivry, R. B., & Pokorny, R. A. (1989). Mechanisms of perceptual timing: Beat-based  
1381 or interval-based judgements? *Psychological Research*, 50, 251–256. <https://doi.org/10.1007/BF00309261>

1382 Keitel, C., Obleser, J., Jessen, S., & Henry, M. J. (2021). Frequency-Specific Effects in Infant  
1383 Electroencephalograms Do Not Require Entrained Neural Oscillations: A Commentary on Köster et al.  
1384 (2019). *Psychological Science*, 32(6), 966–971. <https://doi.org/10.1177/09567976211001317>

1385 King, J.-R., & Dehaene, S. (2014). Characterizing the dynamics of mental representations: the temporal  
1386 generalization method. *Trends in Cognitive Sciences*, 18(4), 203–210.  
1387 <https://doi.org/10.1016/J.TICS.2014.01.002>

1388 Kloosterman, N. A., Kosciessa, J. Q., Lindenberger, U., Fahrenfort, J. J., & Garrett, D. D. (2020). Boosts in  
1389 brain signal variability track liberal shifts in decision bias. *ELife*, 9, 1–22.  
1390 <https://doi.org/10.7554/ELIFE.54201>

1391 Kosciessa, J. Q., Kloosterman, N. A., & Garrett, D. D. (2020). Standard multiscale entropy reflects neural  
1392 dynamics at mismatched temporal scales: What's signal irregularity got to do with it? *PLoS Computational  
1393 Biology*, 16(5), e1007885. <https://doi.org/10.1371/journal.pcbi.1007885>

1394 Kösem, A., Bosker, H. R., Takashima, A., Meyer, A., Jensen, O., & Hagoort, P. (2018). Neural Entrainment  
1395 Determines the Words We Hear. *Current Biology*, 28(18), 2867–2875.e3.  
1396 <https://doi.org/10.1016/j.cub.2018.07.023>

1397 Lange, K. (2009). Brain correlates of early auditory processing are attenuated by expectations for time and pitch.  
1398 *Brain and Cognition*, 69(1), 127–137. <https://doi.org/10.1016/j.bandc.2008.06.004>

1399 Large, E. W. (2008). Resonating to musical rhythm: Theory and experiment. In S. Grondin (Ed.), *Psychology of  
1400 time* (pp. 189–231). Bingley, UK: Emerald Group Publishing. [https://doi.org/10.1016/B978-0-8046-977-5.00006-5](https://doi.org/10.1016/B978-0-8046-977-<br/>1401 5.00006-5)

1402 Large, E. W., Herrera, J. A., & Velasco, M. J. (2015). Neural networks for beat perception in musical rhythm.  
1403 *Frontiers in Systems Neuroscience*, 9(November), 159. <https://doi.org/10.3389/fnsys.2015.00159>

1404 Large, E. W., & Jones, M. R. (1999). The dynamics of attending: how people track time-varying events.  
1405 *Psychological Review*, 106(1), 119–159. <https://doi.org/10.1037/0033-295X.106.1.119>

1406 Large, E. W., & Palmer, C. (2002). Perceiving temporal regularity in music. *Cognitive Science*, 26(1), 1–37.  
1407 [https://doi.org/10.1207/s15516709cog2601\\_1](https://doi.org/10.1207/s15516709cog2601_1)

1408 Law, L. N. C., & Zentner, M. (2012). Assessing Musical Abilities Objectively: Construction and Validation of  
1409 the Profile of Music Perception Skills. *PLoS ONE*, 7(12), e52508.  
1410 <https://doi.org/10.1371/journal.pone.0052508>

1411 Lenc, T., Keller, P. E., Varlet, M., & Nozaradan, S. (2018). Neural tracking of the musical beat is enhanced by

1412 low-frequency sounds. *Proceedings of the National Academy of Sciences*, 115(32), 8221–8226.  
1413 <https://doi.org/10.1073/pnas.1801421115>

1414 Lenc, T., Merchant, H., Keller, P. E., Honing, H., Varlet, M., & Nozaradan, S. (2021). Mapping between sound,  
1415 brain and behaviour: Four-level framework for understanding rhythm processing in humans and non-  
1416 human primates. *Philosophical Transactions of the Royal Society B: Biological Sciences*, 376, 20200325.  
1417 <https://doi.org/10.1098/rstb.2020.0325>

1418 Lenth, R. (2019). emmeans: Estimated Marginal Means, aka Least-Squares Means. R package version 1.4.  
1419 Retrieved from <https://cran.r-project.org/package=emmeans>

1420 Leow, L., & Grahn, J. A. (2014). Neural mechanisms of rhythm perception: Present findings and future  
1421 directions. In H. Merchant & V. de Lafuente (Eds.), *Neurobiology of Interval Timing* (pp. 325–338). New  
1422 York: Springer. <https://doi.org/10.1007/978-1-4939-1782-2>

1423 Lin, W. M., Oetringer, D. A., Bakker-Marshall, I., Emmerzaal, J., Wilsch, A., ElShafei, H. A., ... Haegens, S.  
1424 (2021). No behavioural evidence for rhythmic facilitation of perceptual discrimination. *European Journal  
1425 of Neuroscience*. <https://doi.org/10.1111/ejn.15208>

1426 London, J. (2012). *Hearing in time: Psychological aspects of musical meter*. (2nd ed.). Oxford: Oxford  
1427 University Press.

1428 Los, S. A., & Heslenfeld, D. J. (2005). Intentional and Unintentional Contributions to Nonspecific Preparation:  
1429 Electrophysiological Evidence. *Journal of Experimental Psychology: General*, 134(1), 52–72.  
1430 <https://doi.org/10.1037/0096-3445.134.1.52>

1431 Manning, F. C., Harris, J., & Schutz, M. (2017). Temporal prediction abilities are mediated by motor effector  
1432 and rhythmic expertise. *Experimental Brain Research*, 235(3), 861–871. [https://doi.org/10.1007/s00221-016-4845-8](https://doi.org/10.1007/s00221-<br/>1433 016-4845-8)

1434 Manning, F. C., & Schutz, M. (2013). “Moving to the beat” improves timing perception. *Psychonomic Bulletin  
1435 & Review*, 20, 1133–1139. <https://doi.org/10.3758/s13423-013-0439-7>

1436 Mathewson, K. E., Prudhomme, C., Fabiani, M., Beck, D. M., Lleras, A., & Gratton, G. (2012). Making Waves  
1437 in the Stream of Consciousness: Entraining Oscillations in EEG Alpha and Fluctuations in Visual  
1438 Awareness with Rhythmic Visual Stimulation. *Journal of Cognitive Neuroscience*, 24(12), 2321–2333.  
1439 [https://doi.org/10.1162/jocn\\_a\\_00288](https://doi.org/10.1162/jocn_a_00288)

1440 Matthews, T. E., Thibodeau, J. N. L., Gunther, B. P., & Penhune, V. B. (2016). The Impact of Instrument-  
1441 Specific Musical Training on Rhythm Perception and Production. *Frontiers in Psychology*, 7(February),  
1442 69. <https://doi.org/10.3389/fpsyg.2016.00069>

1443 Mento, G. (2013). The passive CNV: Carving out the contribution of task-related processes to expectancy.  
1444 *Frontiers in Human Neuroscience*, 7(December), 827. <https://doi.org/10.3389/fnhum.2013.00827>

1445 Mento, G. (2017). The role of the P3 and CNV components in voluntary and automatic temporal orienting: A  
1446 high spatial-resolution ERP study. *Neuropsychologia*, 107, 31–40.  
1447 <https://doi.org/10.1016/J.NEUROPSYCHOLOGIA.2017.10.037>

1448 Merchant, H., Grahn, J. A., Trainor, L. J., Rohrmeier, M. A., & Fitch, W. T. (2015). Finding the beat: a neural  
1449 perspective across humans and non-human primates. *Philosophical Transactions of the Royal Society B*,  
1450 370, 20140093. <https://doi.org/10.1098/rstb.2014.0093>

1451 Meyer, L., Sun, Y., & Martin, A. E. (2019). Synchronous, but not entrained: exogenous and endogenous cortical  
1452 rhythms of speech and language processing. *Language, Cognition and Neuroscience*, 1–11.  
1453 <https://doi.org/10.1080/23273798.2019.1693050>

1454 Morillon, B., Schroeder, C. E., Wyart, V., & Arnal, L. H. (2016). Temporal prediction in lieu of periodic  
1455 stimulation. *The Journal of Neuroscience*, 36(8), 2342–2347. [https://doi.org/10.1523/JNEUROSCI.0836-15.2016](https://doi.org/10.1523/JNEUROSCI.0836-<br/>1456 15.2016)

1457 Müllensiefen, D., Gingras, B., Musil, J., & Stewart, L. (2014). The musicality of non-musicians: An index for  
1458 assessing musical sophistication in the general population. *PLoS ONE*, 9(2), e89642.  
1459 <https://doi.org/10.1371/journal.pone.0089642>

1460 Nobre, A. C., & van Ede, F. (2018). Anticipated moments: temporal structure in attention. *Nature Reviews  
1461 Neuroscience*, 19, 34–48. <https://doi.org/10.1038/nrn.2017.141>

1462 Novembre, G., & Iannetti, G. D. (2018). Tagging the musical beat: Neural entrainment or event-related  
1463 potentials? *Proceedings of the National Academy of Sciences*, 115(47), E11002–E11003.  
1464 [https://doi.org/10.1073/pnas.181531115](https://doi.org/10.1073/pnas.1815311115)

1465 Nozaradan, S., Peretz, I., Missal, M., & Mouraux, A. (2011). Tagging the neuronal entrainment to beat and  
1466 meter. *The Journal of Neuroscience*, 31(28), 10234–10240. [https://doi.org/10.1523/JNEUROSCI.0411-11.2011](https://doi.org/10.1523/JNEUROSCI.0411-<br/>1467 11.2011)

1468 Nozaradan, S., Peretz, I., & Mouraux, A. (2012). Selective neuronal entrainment to the beat and meter embedded  
1469 in a musical rhythm. *The Journal of Neuroscience*, 32(49), 17572–17581.  
1470 <https://doi.org/10.1523/JNEUROSCI.3203-12.2012>

1471 O'Reilly, J. X., McCarthy, K. J., Capizzi, M., & Nobre, A. C. (2008). Acquisition of the temporal and ordinal

1472 structure of movement sequences in incidental learning. *Journal of Neurophysiology*, 99, 2731–2735.  
1473 <https://doi.org/10.1152/jn.01141.2007>

1474 Obleser, J., & Kayser, C. (2019). Neural Entrainment and Attentional Selection in the Listening Brain. *Trends in*  
1475 *Cognitive Sciences*, 23(11), 913–926. <https://doi.org/10.1016/J.TICS.2019.08.004>

1476 Oostenveld, R., Fries, P., Maris, E., & Schoffelen, J.-M. (2011). FieldTrip: Open source software for advanced  
1477 analysis of MEG, EEG, and invasive electrophysiological data. *Computational Intelligence and*  
1478 *Neuroscience*, 2011, 156869. <https://doi.org/10.1155/2011/156869>

1479 Palmer, C., & Krumhansl, C. L. (1990). Mental representations for musical meter. *Journal of Experimental*  
1480 *Psychology. Human Perception and Performance*, 16(4), 728–741. Retrieved from  
1481 <http://www.ncbi.nlm.nih.gov/pubmed/2148588>

1482 Pesnot Lerousseau, J., Trébuchon, A., Morillon, B., & Schön, D. (2021). Frequency selectivity of persistent  
1483 cortical oscillatory responses to auditory rhythmic stimulation. *The Journal of Neuroscience*, 41(38),  
1484 7991–8006. <https://doi.org/10.1523/JNEUROSCI.0213-21.2021>

1485 Povel, D.-J., & Essens, P. (1985). Perception of Temporal Patterns. *Music Perception*, 2(4), 411–440.  
1486 <https://doi.org/10.2307/40285311>

1487 Povel, D.-J., & Okkerman, H. (1981). Accents in equitone sequences. *Perception & Psychophysics*, 30(6), 565–  
1488 572. <https://doi.org/10.3758/BF03202011>

1489 Praamstra, P., Kourtis, D., Kwok, H. F., & Oostenveld, R. (2006). Neurophysiology of implicit timing in serial  
1490 choice reaction-time performance. *The Journal of Neuroscience*, 26(20), 5448–5455.  
1491 <https://doi.org/10.1523/JNEUROSCI.0440-06.2006>

1492 R Development Core Team. (2008). *R: A language and environment for statistical computing*. Vienna, Austria:  
1493 R Foundation for Statistical Computing. Retrieved from [www.R-project.org](http://www.R-project.org)

1494 Rimmele, J. M., Morillon, B., Poeppel, D., & Arnal, L. H. (2018). Proactive sensing of periodic and aperiodic  
1495 auditory patterns. *Trends in Cognitive Sciences*, 22(10), 870–882.  
1496 <https://doi.org/10.1016/J.TICS.2018.08.003>

1497 Schmidt-Kassow, M., Schubotz, R. I., & Kotz, S. A. (2009). Attention and entrainment: P3b varies as a function  
1498 of temporal predictability. *NeuroReport*, 20(1), 31–36. <https://doi.org/10.1097/WNR.0b013e32831b4287>

1499 Schroeder, C. E., & Lakatos, P. (2009a). Low-frequency neuronal oscillations as instruments of sensory  
1500 selection. *Trends in Neurosciences*, 32(1), 9–18. <https://doi.org/10.1016/j.tins.2008.09.012>

1501 Schroeder, C. E., & Lakatos, P. (2009b). The Gamma Oscillation: Master or Slave? *Brain Topography*, 22, 24–  
1502 26. <https://doi.org/10.1007/s10548-009-0080-y>

1503 Schultz, B. G., Stevens, C. J., Keller, P. E., & Tillmann, B. (2013). The implicit learning of metrical and  
1504 nonmetrical temporal patterns. *The Quarterly Journal of Experimental Psychology*, 66(2), 360–380.  
1505 <https://doi.org/10.1080/17470218.2012.712146>

1506 Shalev, N., Nobre, A. C., & van Ede, F. (2019). Time for What? Breaking Down Temporal Anticipation. *Trends*  
1507 *in Neurosciences*, 42(6), 373–374. <https://doi.org/10.1016/J.TINS.2019.03.002>

1508 Stefanics, G., Hangya, B., Hernádi, I., Winkler, I., Lakatos, P., & Ulbert, I. (2010). Phase Entrainment of Human  
1509 Delta Oscillations Can Mediate the Effects of Expectation on Reaction Speed. *The Journal of*  
1510 *Neuroscience*, 30(41), 13578–13585. <https://doi.org/10.1523/JNEUROSCI.0703-10.2010>

1511 Sun, Y., Michalareas, G., & Poeppel, D. (2021). The impact of phase entrainment on auditory detection is highly  
1512 variable: Revisiting a key finding. *European Journal of Neuroscience*, (June), 1–18.  
1513 <https://doi.org/10.1111/ejn.15367>

1514 Tal, I., Large, E. W., Rabinovitch, E., Wei, Y., Schroeder, C. E., Poeppel, D., & Golumbic, E. Z. (2017). Neural  
1515 entrainment to the beat: The “missing-pulse” phenomenon. *The Journal of Neuroscience*, 37(26), 6331–  
1516 6341. <https://doi.org/10.1523/JNEUROSCI.2500-16.2017>

1517 Teki, S., Grube, M., Kumar, S., & Griffiths, T. D. (2011). Distinct neural substrates of duration-based and beat-  
1518 based auditory timing. *The Journal of Neuroscience*, 31(10), 3805–3812.  
1519 <https://doi.org/10.1523/JNEUROSCI.5561-10.2011>

1520 Tichko, P., & Large, E. W. (2019). Modeling infants’ perceptual narrowing to musical rhythms: neural  
1521 oscillation and Hebbian plasticity. *Annals of the New York Academy of Sciences*, 1453(April), 125–139.  
1522 <https://doi.org/10.1111/nyas.14050>

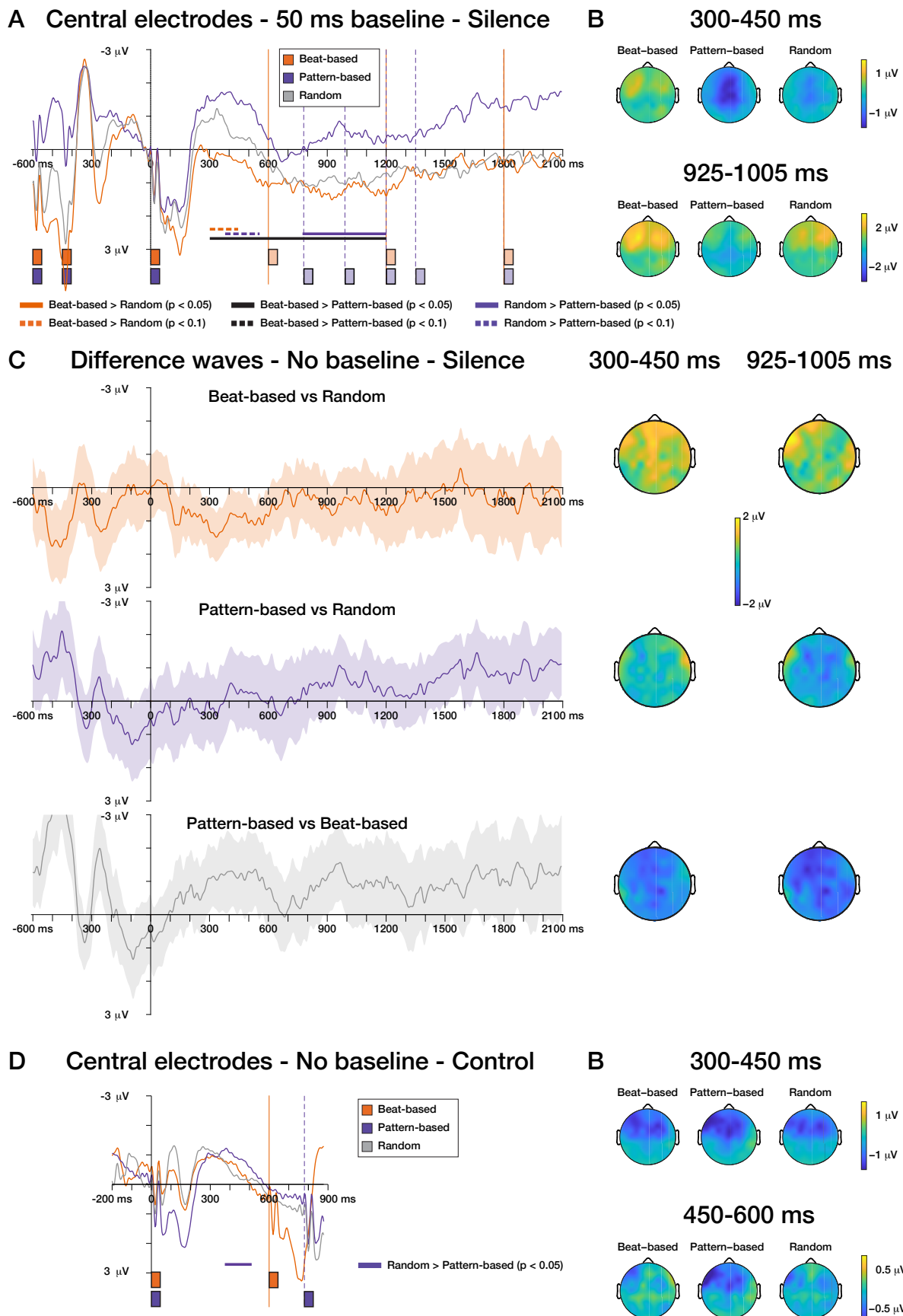
1523 van Atteveldt, N., Musacchia, G., Zion-Golumbic, E., Sehatpour, P., Javitt, D. C., & Schroeder, C. E. (2015).  
1524 Complementary fMRI and EEG evidence for more efficient neural processing of rhythmic vs.  
1525 unpredictably timed sounds. *Frontiers in Psychology*, 6(OCT), 1–11.  
1526 <https://doi.org/10.3389/fpsyg.2015.01663>

1527 van Bree, S., Sohoglu, E., Davis, M. H., & Zoefel, B. (2021). Sustained neural rhythms reveal endogenous  
1528 oscillations supporting speech perception. *PLOS Biology*, 19(2), e3001142.  
1529 <https://doi.org/10.1371/journal.pbio.3001142>

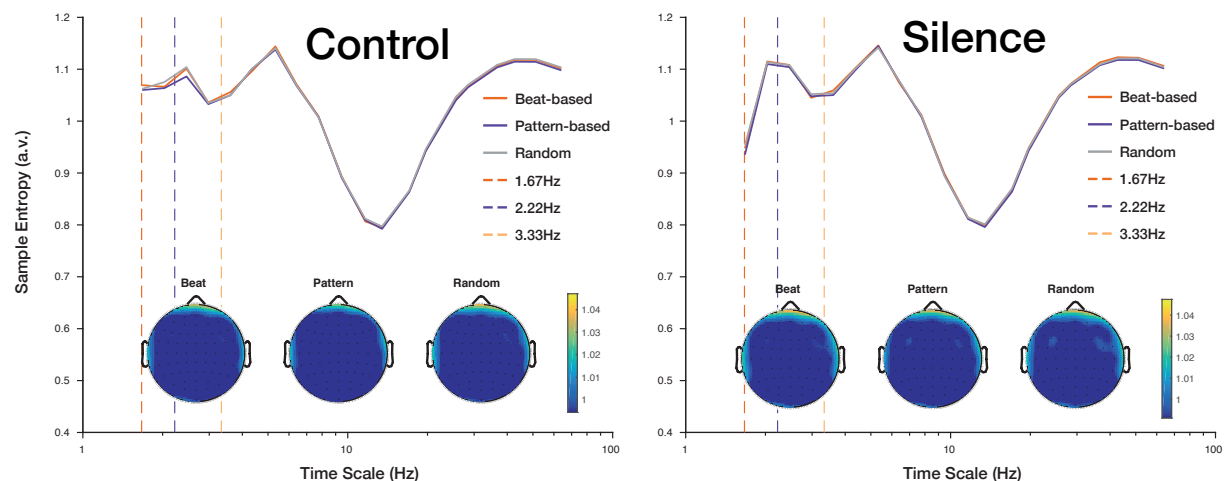
1530 van der Weij, B., Pearce, M. T., & Honing, H. (2017). A probabilistic model of meter perception: simulating  
1531 enculturation. *Frontiers in Psychology*, 8(May), 824. <https://doi.org/10.3389/fpsyg.2017.00824>

1532 Vuust, P., Pallesen, K. J., Bailey, C., Van Zuijen, T. L., Gjedde, A., Roepstorff, A., & Østergaard, L. (2005). To  
1533 musicians, the message is in the meter: Pre-attentive neuronal responses to incongruent rhythm are left-  
1534 lateralized in musicians. *NeuroImage*, 24(2), 560–564. <https://doi.org/10.1016/j.neuroimage.2004.08.039>  
1535 Wagenmakers, E.-J., Love, J., Marsman, M., Jamil, T., Ly, A., Verhagen, J., ... Morey, R. D. (2018). Bayesian  
1536 inference for psychology. Part II: Example applications with JASP. *Psychonomic Bulletin & Review*,  
1537 25(1), 58–76. <https://doi.org/10.3758/s13423-017-1323-7>  
1538 Waschke, L., Kloosterman, N. A., Obleser, J., & Garrett, D. D. (2021). Behavior needs neural variability.  
1539 *Neuron*, 109(5), 751–766. <https://doi.org/10.1016/j.neuron.2021.01.023>  
1540 Wilsch, A., Mercier, M. R., Obleser, J., Schroeder, C. E., & Haegens, S. (2020). Spatial Attention and Temporal  
1541 Expectation Exert Differential Effects on Visual and Auditory Discrimination. *Journal of Cognitive*  
1542 *Neuroscience*, 32(8), 1562–1576. [https://doi.org/10.1162/jocn\\_a\\_01567](https://doi.org/10.1162/jocn_a_01567)  
1543 Wollman, I., & Morillon, B. (2018). Organizational principles of multidimensional predictions in human  
1544 auditory attention. *Scientific Reports*, 8(1), 13466. <https://doi.org/10.1038/s41598-018-31878-5>  
1545 Zalta, A., Petkoski, S., & Morillon, B. (2020). Natural rhythms of periodic temporal attention. *Nature*  
1546 *Communications*, 11(1), 1051. <https://doi.org/10.1038/s41467-020-14888-8>  
1547 Zoefel, B., ten Oever, S., & Sack, A. T. (2018). The Involvement of Endogenous Neural Oscillations in the  
1548 Processing of Rhythmic Input: More Than a Regular Repetition of Evoked Neural Responses. *Frontiers in*  
1549 *Neuroscience*, 12, 95. <https://doi.org/10.3389/fnins.2018.00095>  
1550 Zoefel, B., & Vanrullen, R. (2017). Oscillatory mechanisms of stimulus processing and selection in the visual  
1551 and auditory systems: State-of-the-art, speculations and suggestions. *Frontiers in Neuroscience*, 11(May),  
1552 296. <https://doi.org/10.3389/fnins.2017.00296>  
1553  
1554  
1555  
1556  
1557  
1558

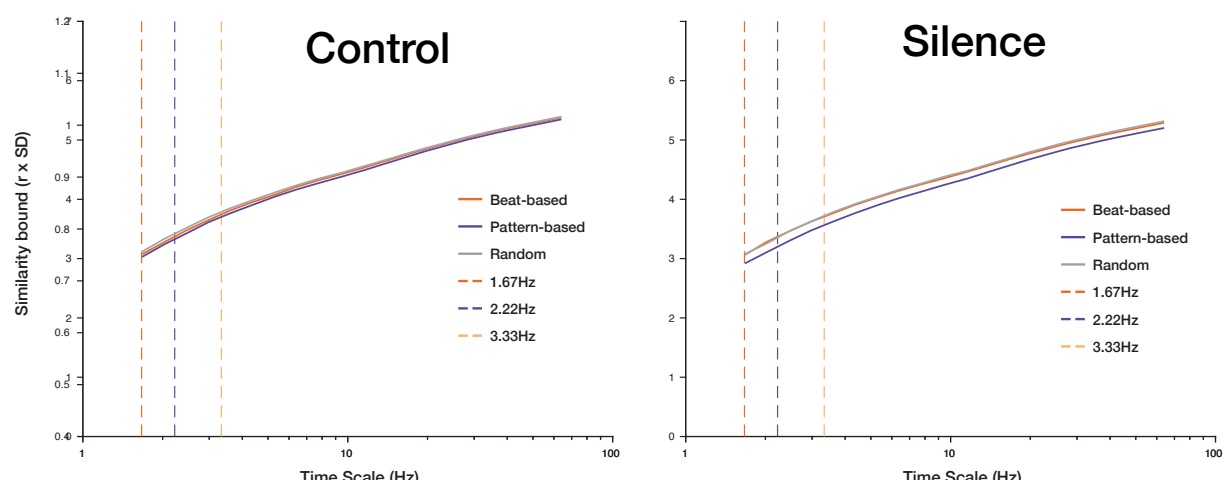
**Supplementary materials for “A silent disco: Persistent entrainment of low-frequency neural oscillations underlies beat-based, but not pattern-based temporal expectations”**  
*(Bouwer, Fahrenfort, Millard, Kloosterman, & Slagter, 2022)*



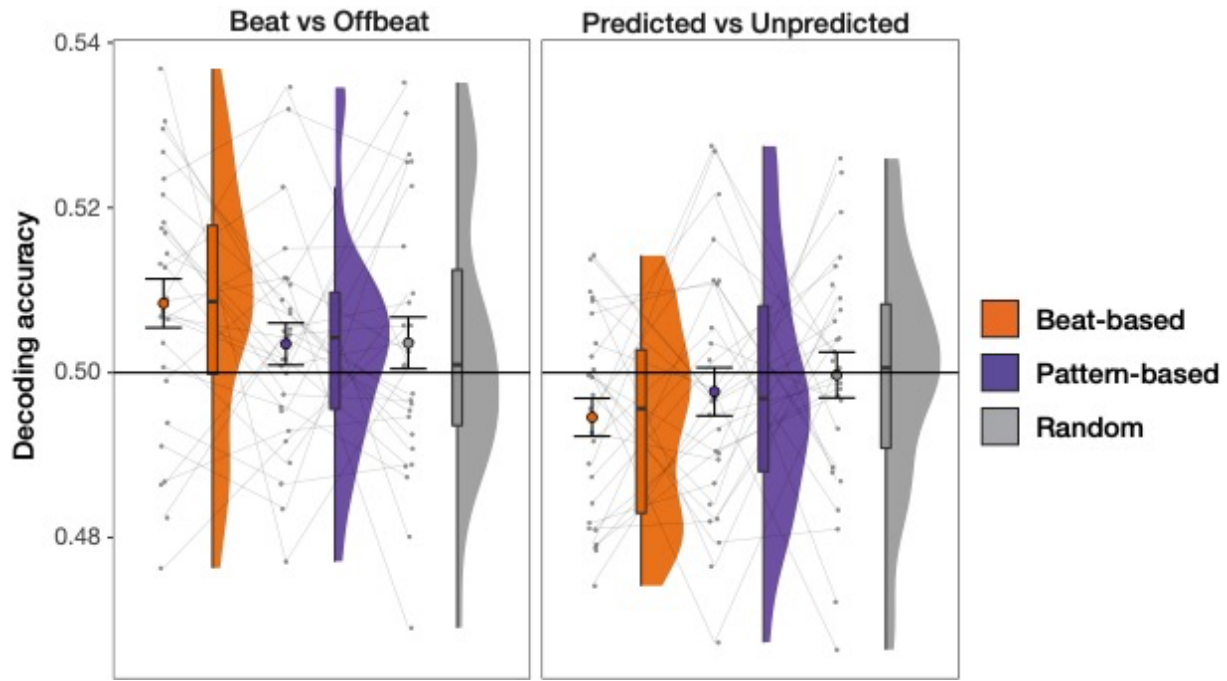
**Supplementary Figure 1. ERPs with traditional 50 ms baseline and difference waves.** A) With the more traditional pre-cue baseline, there was a trend for the random condition to elicit a more negative deflection than the beat-based condition ( $p = 0.058$ , 300 – 446 ms) and for the pattern-based condition to elicit a more negative deflection than the random condition (early window:  $p = 0.083$ , 380 – 551 ms; later window:  $p = 0.022$ , 774 – 1200 ms). Note that a significant cluster spanning the entire analysis window of 300 – 1200 ms was found when comparing between the pattern-based and beat-based condition with baseline correction ( $p = 0.011$ ), indicative of a possible overall shift due to the baseline correction. However, the overall picture stays the same as when not using a baseline, a negative deflection can be seen around 300-450 ms after the last sound onset for the pattern-based and random, but not the beat-based condition. B) Scalp distributions for windows with a significant cluster (see also Figure 5). C) Difference waves depicting condition differences and the 95% confidence interval around the mean difference waveforms. The scalp distributions similarly depict condition differences. D) Evoked potential showing the ERPs during sound presentation. Time 0 here is the presentation of a sound, with the next sound being presented at 600 (beat-based condition) or 780 ms (pattern-based and random condition). As in the silence window, a negative deflection can be observed, which was larger for the pattern-based than random condition ( $p = 0.039$ ), and peaks around 350 ms after the onset of the previous sound. The difference between the pattern-based and beat-based condition here did not reach significance ( $p = 0.1$ ), likely because of the noisy baseline.



**Supplementary Figure 2. MMSE after highpass filtering at 5 Hz.** Here, all differences between conditions are eliminated by the highpass filtering.



**Supplementary Figure 3. Similarity bounds used to calculate MMSE values mirror the condition differences.** This finding suggests that condition differences found in the entropy measure, with higher entropy for the pattern-based than random condition in the silence window, may be due to overall variability differences, with lower variability for the pattern-based than random condition, rather than differences in entropy of the signal.



**Supplementary Figure 4. Above chance decoding for beat vs offbeat time points only after listening to beat-based sequences.** For the within-condition decoding analysis, we used a classification algorithm to differentiate between times that were expected or unexpected based on the beat (on the beat: 600 and 1200 ms after the onset of the last tone; offbeat: 780 and 885 ms after the onset of the last tone) or pattern (predicted: 780 and 1200 ms after the onset of the last tone; unpredicted: 600 and 880 ms after the onset of the last tone). The graphs depict the average classification accuracy in a 100 ms time window centered on these expected and unexpected time points in the silence window. Here, the beat-offbeat comparison should yield better decoding if preceded by the beat-based sequences, while the predicted-unpredicted comparison should be decoded better if preceded by the pattern-based sequences. Only decoding of beat vs offbeat positions after the beat-based sequences yielded above-chance decoding ( $t_{26} = 2.84, p = 0.009$ ). None of the other comparisons lead to decoding above chance (all  $p > 0.18$ ), but decoding of predicted vs unpredicted positions in the beat-based condition did yield below-chance decoding ( $p = 0.026$ ). However, a subsequent ANOVA comparing decoding of beat against offbeat positions in all three conditions showed that decoding was not significantly better for the beat-based condition than the other conditions (effect of condition in the silence:  $\chi^2 = 2.1, p = 0.35$ ). Like for the other analyses, there were larger differences between participants, and decoding, while above chance, did not exceed 0.55 accuracy. As for the other EEG measures, the difference in decoding accuracy between the beat-based and random condition, and the pattern-based and random condition did not depend on musical training (both  $p > 0.21$ ).

**Supplementary Table 1.** Simple effects per position from the full models, comparing three conditions. All *p*-values have been Bonferroni corrected for 18 (Experiment 1) or 9 (Experiment 2) comparisons.

Position	Contrast	Experiment 1				Experiment 2			
		Estimate	SE	Z ratio	<i>p</i>	Estimate	SE	Z ratio	<i>p</i>
600 ms	Random – Pattern	2.4	0.09	26.2	<.0001				
	Random – Beat	-1.2	0.09	13.3	<.0001				
	Pattern - Beat	-3.5	0.09	-38.3	<.0001				
780 ms	Random – Pattern	-0.3	0.09	-2.9	0.058				
	Random – Beat	1.6	0.09	18.3	<.0001				
	Pattern - Beat	1.8	0.09	20.7	<.0001				
885 ms	Random – Pattern	-0.1	0.09	-1.6	1				
	Random – Beat	1.5	0.09	17.0	<.0001				
	Pattern - Beat	1.6	0.09	18.4	<.0001				
990 ms	Random – Pattern	0.1	0.09	1.1	1	0.6	0.1	4.8	<.0001
	Random – Beat	1.4	0.09	16.2	<.0001	1.4	0.1	11.4	<.0001
	Pattern - Beat	1.3	0.09	15.0	<.0001	0.8	0.1	6.5	<.0001
1200 ms	Random – Pattern	0.6	0.08	7.5	<.0001	0.2	0.1	1.6	0.92
	Random – Beat	-0.3	0.09	-3.7	0.004	0.1	0.1	0.9	1
	Pattern - Beat	-1.0	0.09	-10.9	<.0001	-0.1	0.1	-0.7	1
1485 ms	Random – Pattern	0.5	0.09	5.2	<.0001	-0.5	0.1	-4.4	<.0001
	Random – Beat	0.6	0.09	6.5	<.0001	0.4	0.1	3.2	0.011
	Pattern - Beat	0.1	0.09	1.3	1	0.9	0.1	7.5	<.0001

**Supplementary Table 2.** Simple effects per condition from the baseline corrected model, using the random condition as baseline, for all positions. All *p*-values have been Bonferroni corrected for 30 (Experiment 1) or 6 (Experiment 2) comparisons.

Condition	Contrast	Experiment 1				Experiment 2			
		Estimate	SE	Z ratio	<i>p</i>	Estimate	SE	Z ratio	<i>p</i>
Beat-based	600 ms - 780 ms	2.3	0.08	28.7	<.0001				
	600 ms - 885 ms	2.2	0.08	27.8	<.0001				
	600 ms - 990 ms	2.1	0.08	27.0	<.0001				
	600 ms - 1200 ms	0.6	0.08	6.9	<.0001				
	600 ms - 1485 ms	1.5	0.08	18.0	<.0001				
	780 ms - 885 ms	-0.1	0.08	-1.3	1				
	780 ms - 990 ms	-0.2	0.08	-1.9	1				
	780 ms - 1200 ms	-1.8	0.08	-21.3	<.0001				
	780 ms - 1485 ms	-0.9	0.08	-10.5	<.0001				
	885 ms - 990 ms	-0.1	0.08	-0.7	1				
	885 ms - 1200 ms	-1.7	0.08	-20.3	<.0001				
	885 ms - 1485 ms	-0.8	0.08	-9.4	<.0001				
	990 ms - 1200 ms	-1.6	0.08	-19.5	<.0001	-1.1	0.1	-9.6	<.0001
	990 ms - 1485 ms	-0.7	0.08	-8.7	<.0001	-0.9	0.1	-7.9	<.0001
	1200 ms - 1485 ms	0.9	0.08	10.9	<.0001	0.2	0.1	1.8	0.46
Pattern-based	600 ms - 780 ms	-2.3	0.09	-27.0	<.0001				
	600 ms - 885 ms	-2.2	0.08	-26.4	<.0001				
	600 ms - 990 ms	-2.1	0.08	-24.8	<.0001				
	600 ms - 1200 ms	-1.7	0.08	-20.2	<.0001				
	600 ms - 1485 ms	-1.7	0.09	-20.3	<.0001				
	780 ms - 885 ms	0.1	0.08	1.0	1				
	780 ms - 990 ms	0.2	0.08	3.0	0.080				
	780 ms - 1200 ms	0.6	0.08	7.6	<.0001				
	780 ms - 1485 ms	0.6	0.08	6.9	<.0001				
	885 ms - 990 ms	0.2	0.08	2.0	1				
	885 ms - 1200 ms	0.5	0.08	6.7	<.0001				
	885 ms - 1485 ms	0.5	0.08	6.0	<.0001				
	990 ms - 1200 ms	0.4	0.08	4.7	<.0001	-0.3	0.1	-2.9	0.022
	990 ms - 1485 ms	0.3	0.08	4.1	0.001	-0.9	0.1	-8.3	<.0001
	1200 ms - 1485 ms	0.0	0.08	-0.5	1.00	-0.6	0.1	-5.4	<.0001

## Supplementary Methods: MSE computation

To compute entropy, epochs were concatenated. Sample entropy was then calculated by taking the following steps:

1. In each time series, a template is selected, consisting of  $m$  samples. The calculation of entropy is an iterative process, using each sample in the time series as a starting point for the template once.
2. Throughout the time series, the algorithm searches for patterns that match the template pattern. A section of samples is considered a match if it resembles the template pattern enough to fall within a set boundary, which is defined as  $r \times \text{SD}$  (the similarity bound).
3. The number of pattern matches is counted.
4. Subsequently, the same procedure is followed for patterns of  $m + 1$  samples long.
5. For the total counts of pattern matches throughout the time series, sample entropy is then calculated as the logarithm of the ratio between pattern matches of length  $m$  and pattern matches of length  $m + 1$ .

Thus, sample entropy reflects the proportion of patterns in the time series that stays similar when an extra sample is added to the pattern. Here, we used  $m = 2$  and  $r = 0.5$ , as was done previously for EEG data (Kloosterman, Kosciessa, Lindenberger, Fahrenfort, & Garrett, 2020).

Sample entropy is then repeated for multiple timescales, to account for contributions of both low and high frequency neural activity. The time series is coarsened step by step, by taking the average of a group of adjacent samples with step-wise increasing group size. This means that long, or coarse, timescales are equivalent to low frequency activity. For example, at a sampling rate of 256 Hz, a timescale of 4 (e.g., averaged over four adjacent samples, or 15.6 ms) is roughly the equivalent of looking at activity at 64 Hz, while a timescale of 153 at that sample rate corresponds to averaging over 598 ms, or the equivalent of activity at roughly 1.67 Hz. Here, we used twenty timescales ranging from 4 till 153, with 153 being the maximum timescale given the length of an epoch of 1800 ms (e.g., one epoch equals 460 samples, but

since entropy is calculated on patterns of 2 and 3 samples, the maximum coarsening to retain the possibility of having a 3-sample pattern is by averaging over 153 samples). Similarity bounds were recomputed for each time scale (Kloosterman et al., 2020; Kosciessa, Kloosterman, & Garrett, 2020). To control for the contribution of delta, we repeated the analysis on high-pass filtered data (5 Hz).

### **Supplementary methods: Within condition decoding**

The initial decoding analysis yielded large effects that may be task-related, and individual differences in phase and metrical level attended to may have additionally hampered finding condition differences at the group level. Therefore, we ran an additional decoding analysis in which we decoded expected and unexpected positions against each other within each condition. For this analysis, we only included frontocentral electrodes (C1, C2, C3, C4, Cz, FC1, FC2, FC3, FC4, FCz, F1, F2, F3, F4, Fz), which were the same electrodes that showed the largest P1 responses to the initial sounds of the sequences, indicative of representing the auditory cortex. Here, we defined time points in the silence as expected or unexpected based on the rhythmic sequences. To equate the choice of expected and unexpected time points as much as possible in terms of number of time points included and distance between time points, we used times that were also used in the probe tone experiment: 600, 780, 885, and 1200 ms. For beat-based sequences, time points 600 and 1200 were expected (on the beat), while time points 780 and 885 were unexpected (offbeat). The same time points take on a different meaning if preceded by the pattern-based sequences. Then, 780 and 1200 ms are considered expected (predictable based on the pattern), while both 600 and 885 ms are unexpected (unpredictable based on the pattern). For all conditions, we examined whether we could classify above chance whether a time window of 100 ms centered on the time point of interest was an expected or unexpected moment in time. As for the first decoding analysis, the data were resampled to improve signal to noise, here to 128 Hz to retain enough data points in the 100 ms window for analysis. After the decoding, we extracted the average classification accuracy for the 100 ms time window to test significance for each condition separately against chance level, using t-tests against 0.5, and between conditions in the silence, using a repeated measures

ANOVA, with condition as an independent factor, a random intercept for participant, and decoding accuracy as the dependent variable.

## References

Kloosterman, N. A., Kosciessa, J. Q., Lindenberger, U., Fahrenfort, J. J., & Garrett, D. D. (2020). Boosts in brain signal variability track liberal shifts in decision bias. *ELife*, 9, 1–22. <https://doi.org/10.7554/ELIFE.54201>

Kosciessa, J. Q., Kloosterman, N. A., & Garrett, D. D. (2020). Standard multiscale entropy reflects neural dynamics at mismatched temporal scales: What's signal irregularity got to do with it? *PLoS Computational Biology*, 16(5), e1007885. <https://doi.org/10.1371/journal.pcbi.1007885>